Charting the low-loss region in Electron Energy Loss Spectroscopy with machine learning

Laurien Roest

October 1st, 2020

Committee members:

Dr. S. Conesa-Boj	Supervisor, TU Delft (QN)
Dr. E. Greplova	TU Delft (QN)
Dr. Ir. J.P. Hoogenboom	TU Delft (ImPhys)

Scientific output

- **First-author paper**

Charting the low-loss region in Electron Energy Loss Spectroscopy with machine learning, Laurien I. Roest, Sabrya E. van Heijst, Louis Maduro, Juan Rojo, and Sonia Conesa-Boj, arXiv:2009.05050
Submitted to: Ultramicroscopy

- **Co-author paper**

Fingerprinting 2H/3R Polytypism in WS2 Nanoflowers from Plasmons and Excitons to Phonons, Sabrya E. van Heijst, Mukai Masaki, E. Okunishi, H. Kurata, Laurien I. Roest, Louis Maduro, Juan Rojo, and Sonia Conesa-Boj, arXiv:2009.08477

- **Open-source Python package**

EELSfitter, made available at GitHub

TEM and EELS

Transmission Electron Microscopy & Electron Energy Loss Spectroscopy

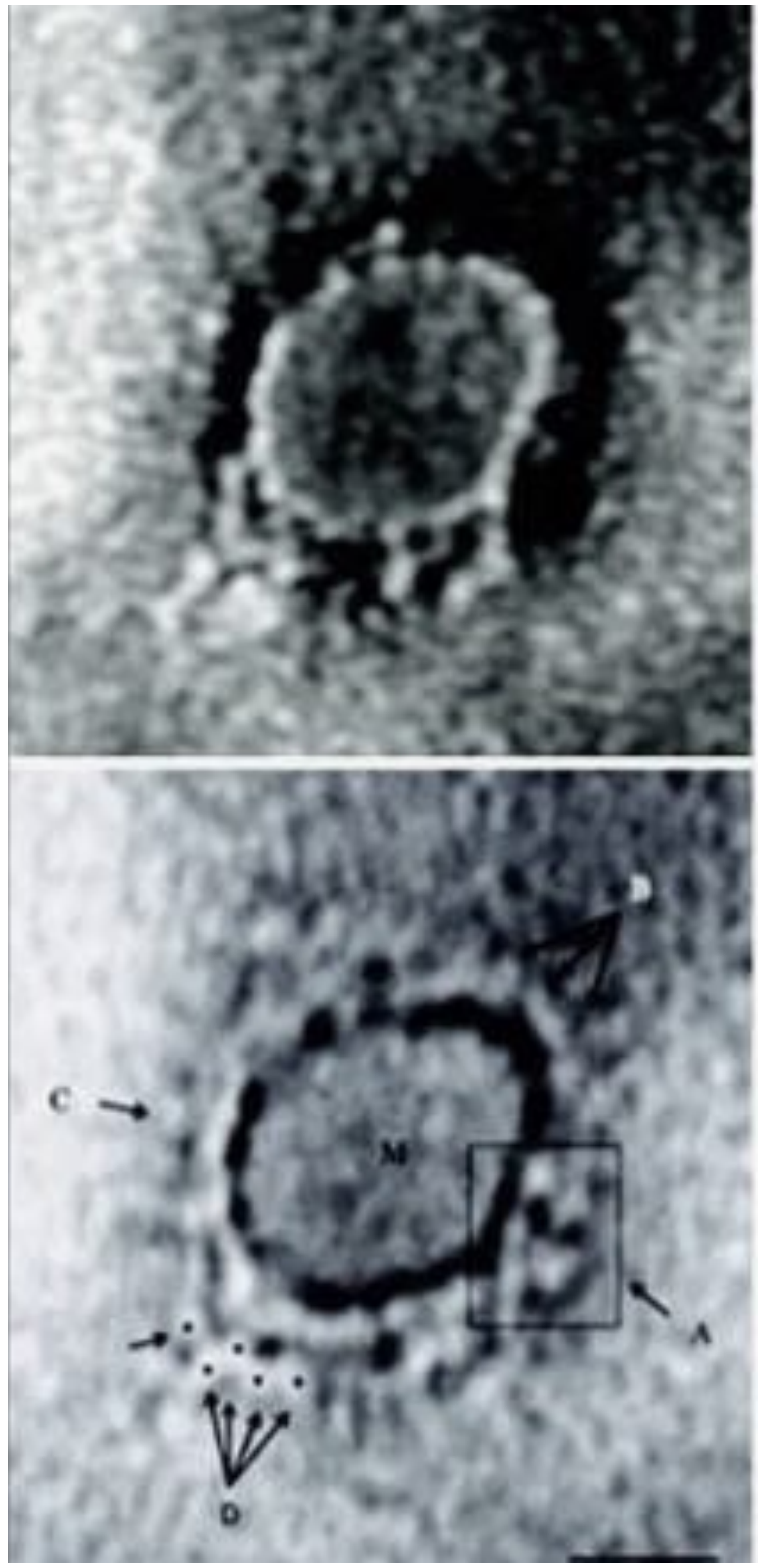

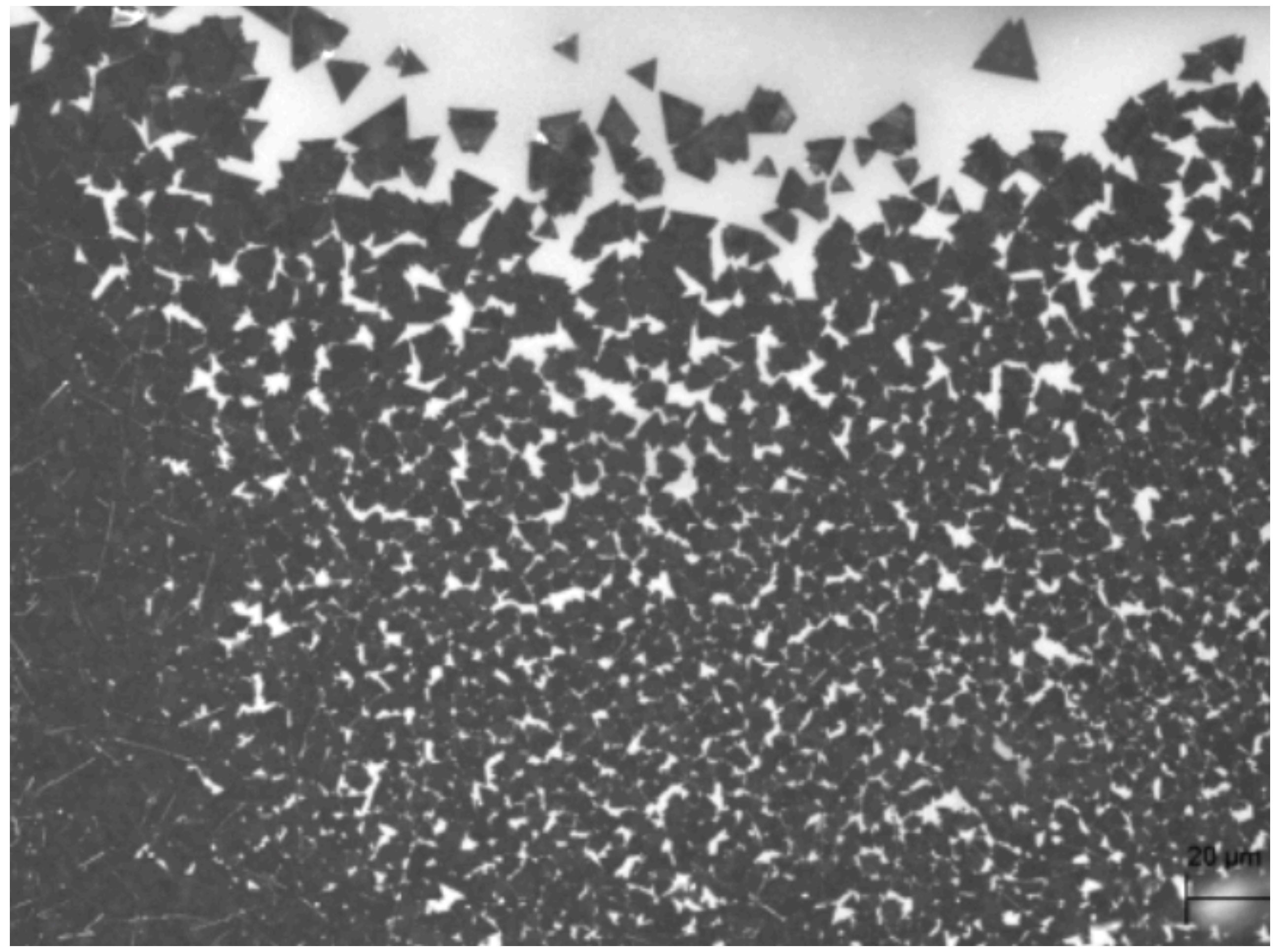

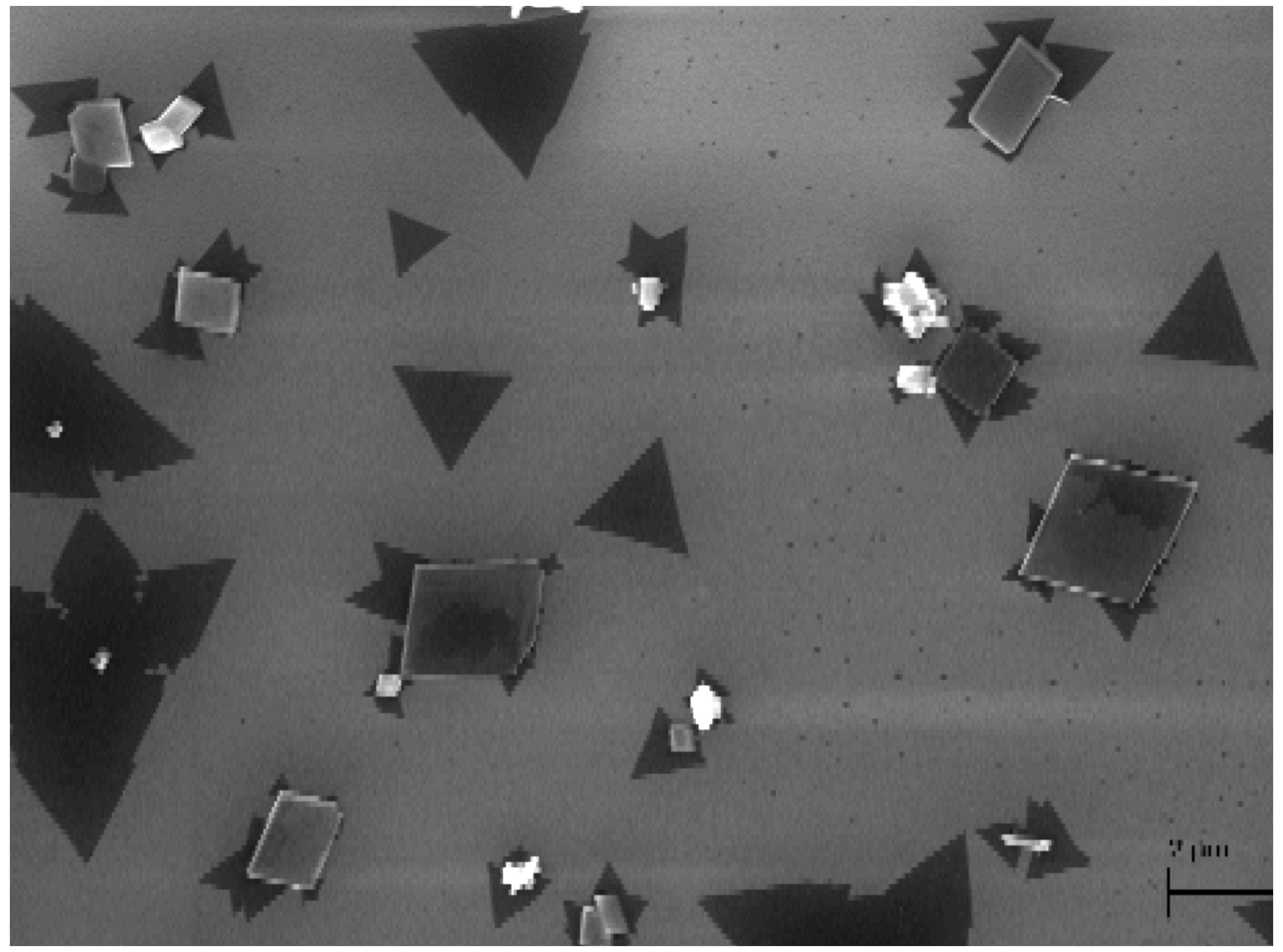

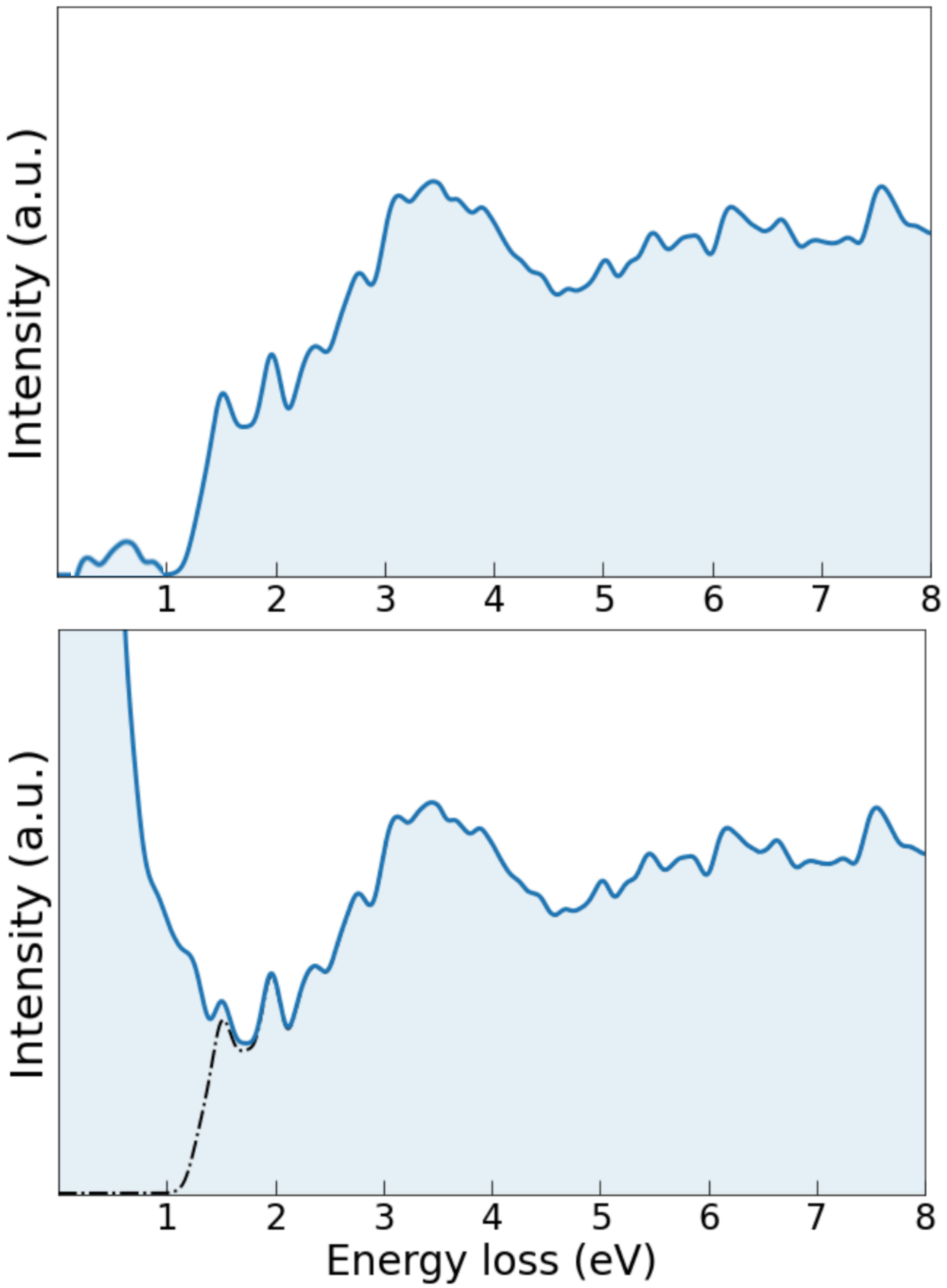

Two-dimensional (2D) materials

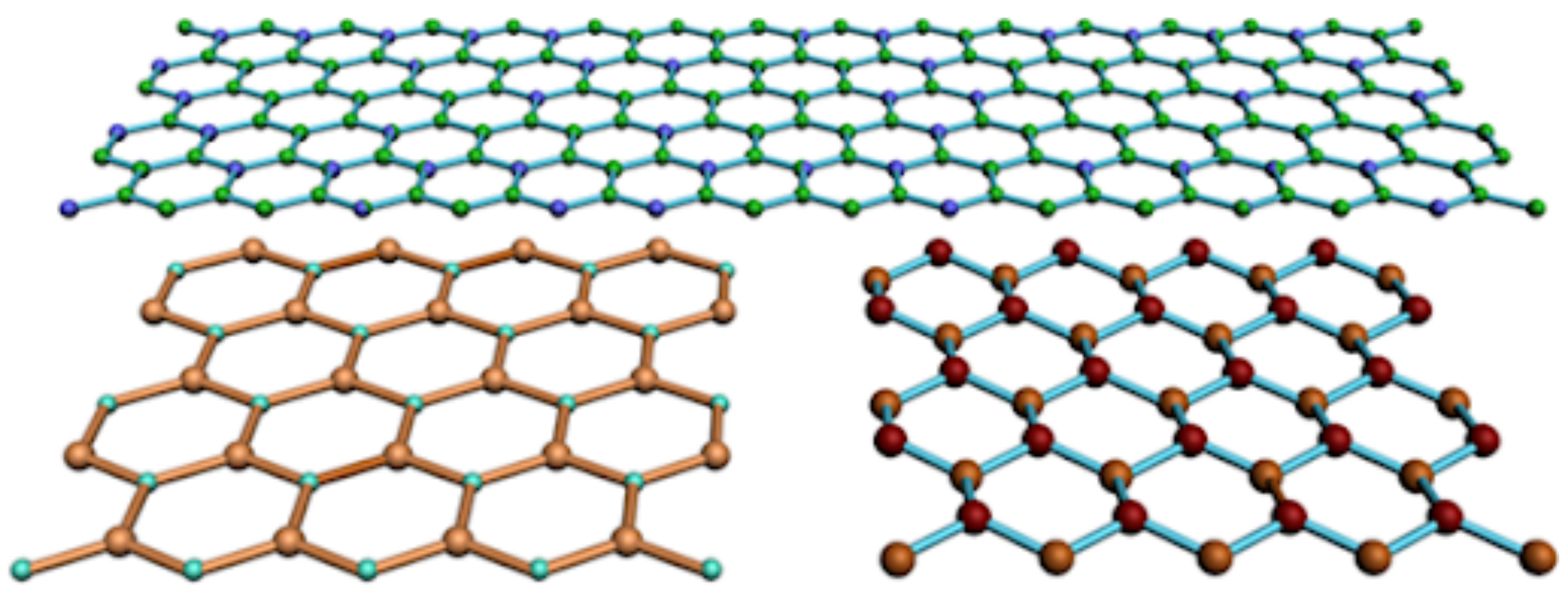

[4]

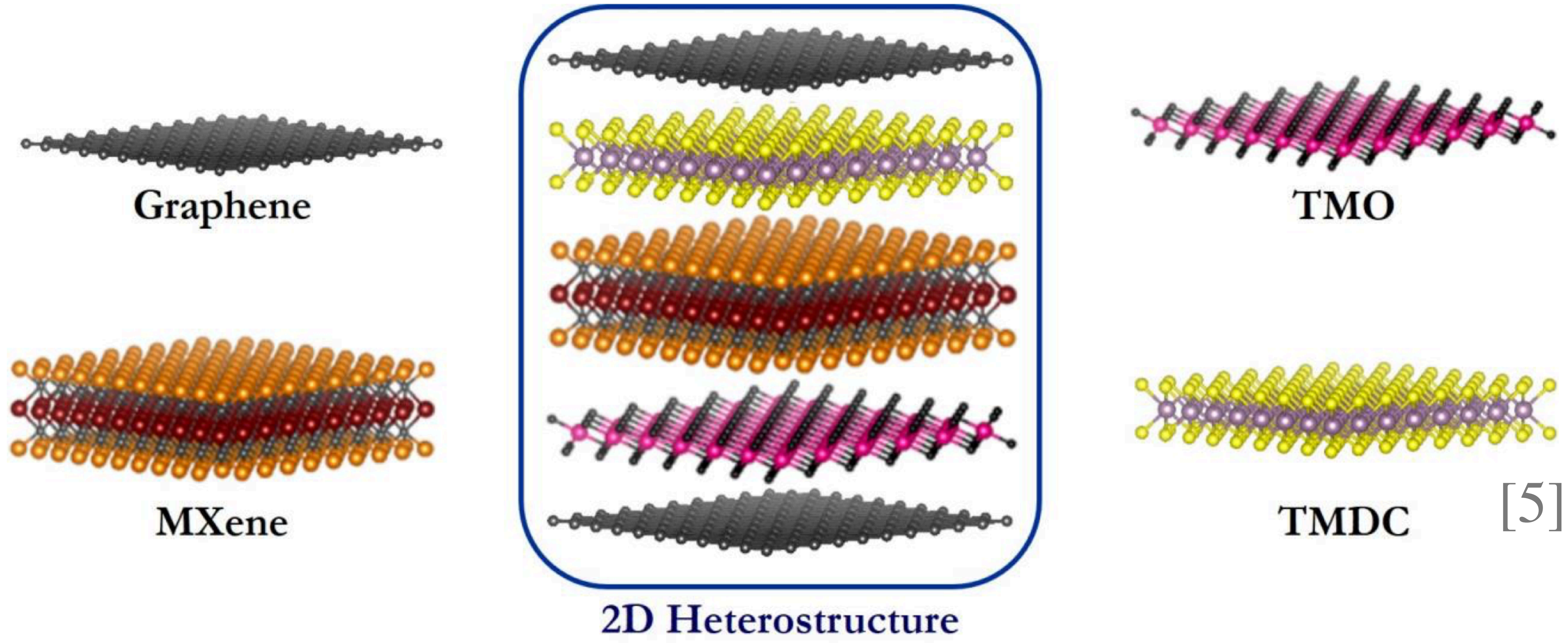

[5]

- Fully functional down to a single layer
- Tunable electronic properties

Vertically stacking different 2D sheets yields **2D heterostructures**

Many possible variations based on:
- Stacking sequence
- Orientation

Transition Metal Dichalcogenides (TMDs)

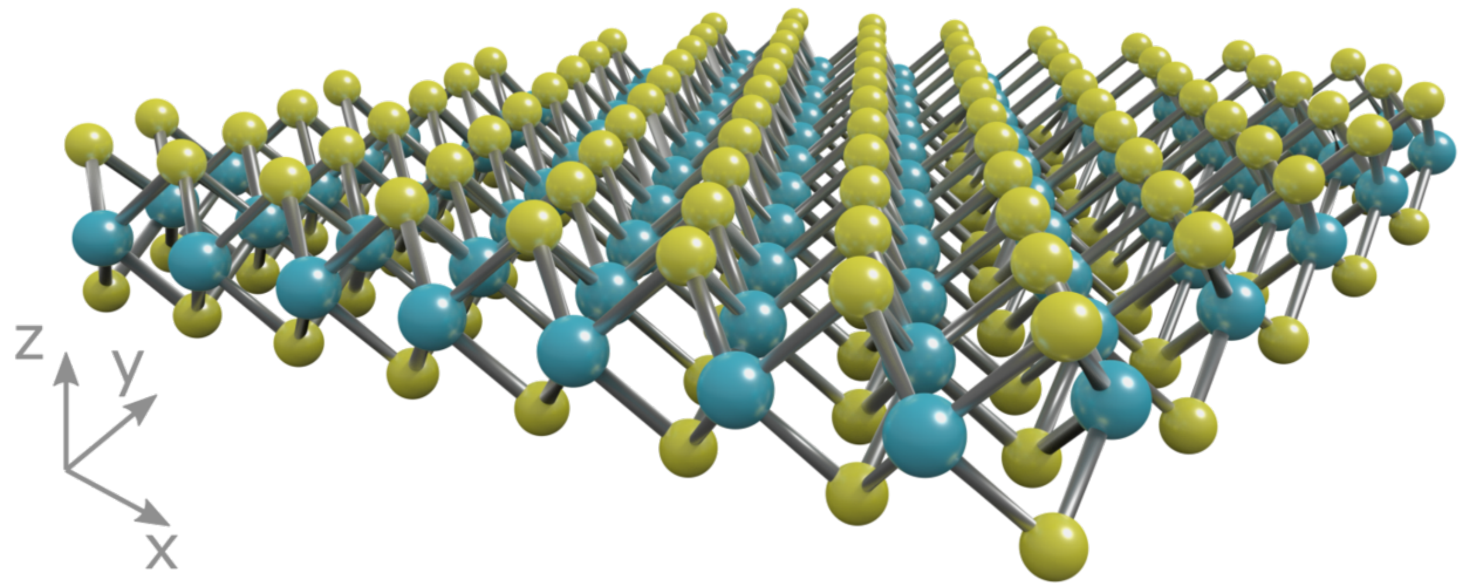

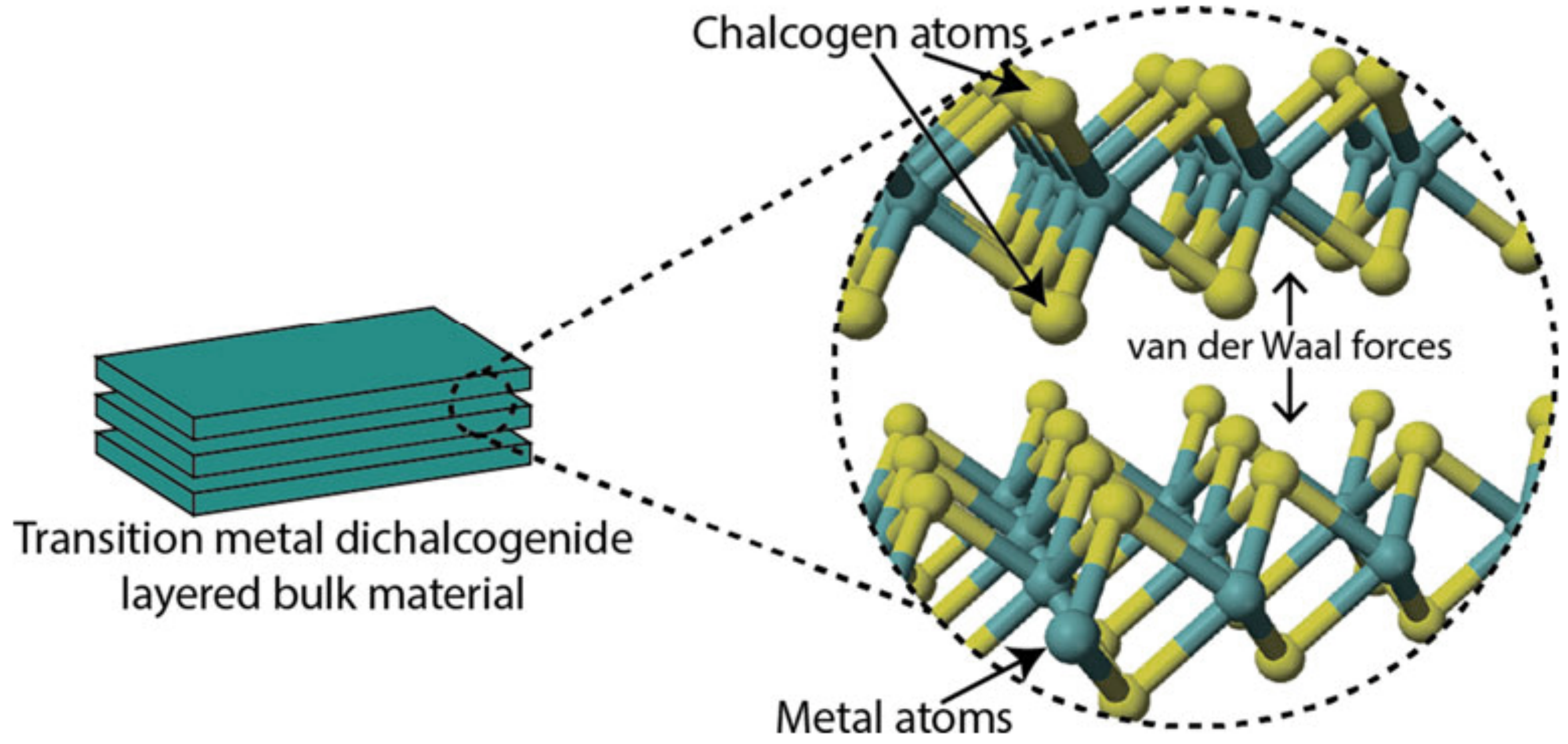

Sandwich structure X-M-X

- Transition metal (M)
- Chalcogen (X)

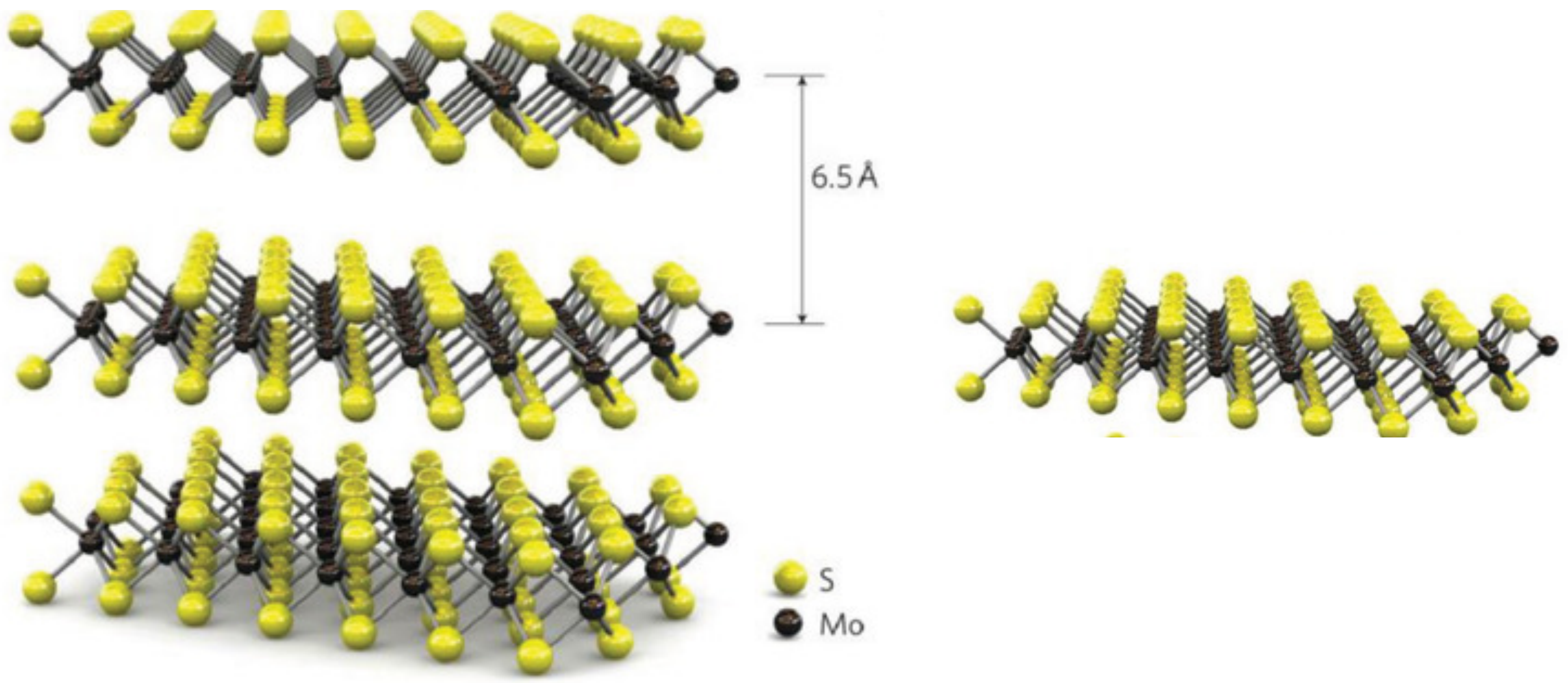

Observed physics changes with:

- Polytype
- Thickness

When TMDs are thinned down, an **direct-to-indirect bandgap transition** occurs

Electron Energy Loss Spectroscopy (EELS)

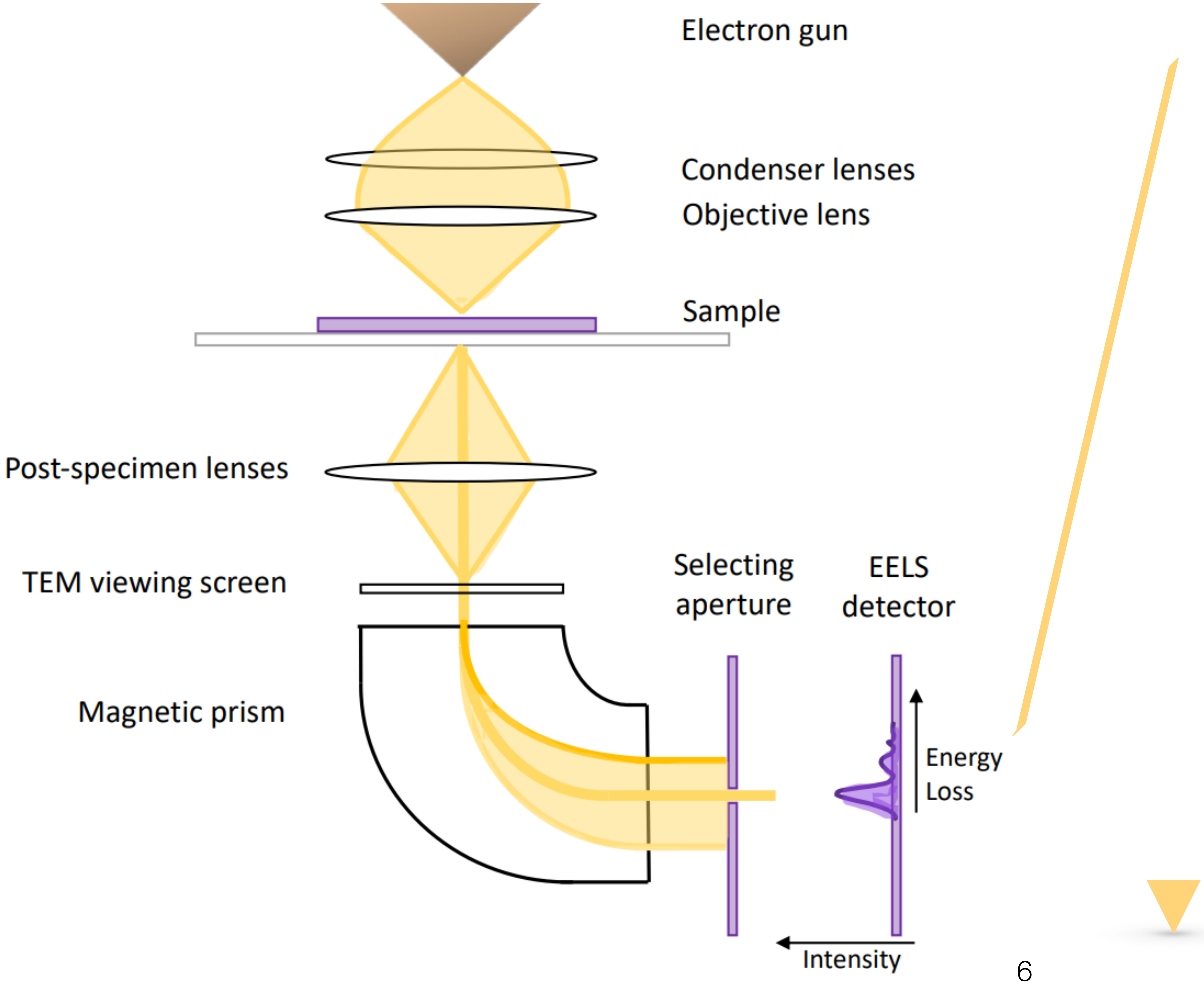

- Monoenergetic electron beam
- Interaction with the sample
  Elastic: $\Delta E = 0$
  Inelastic: $\Delta E \neq 0$
- Difference in energy leads to more/less deflection
- Sorted by their energy loss

Electron Energy Loss spectra

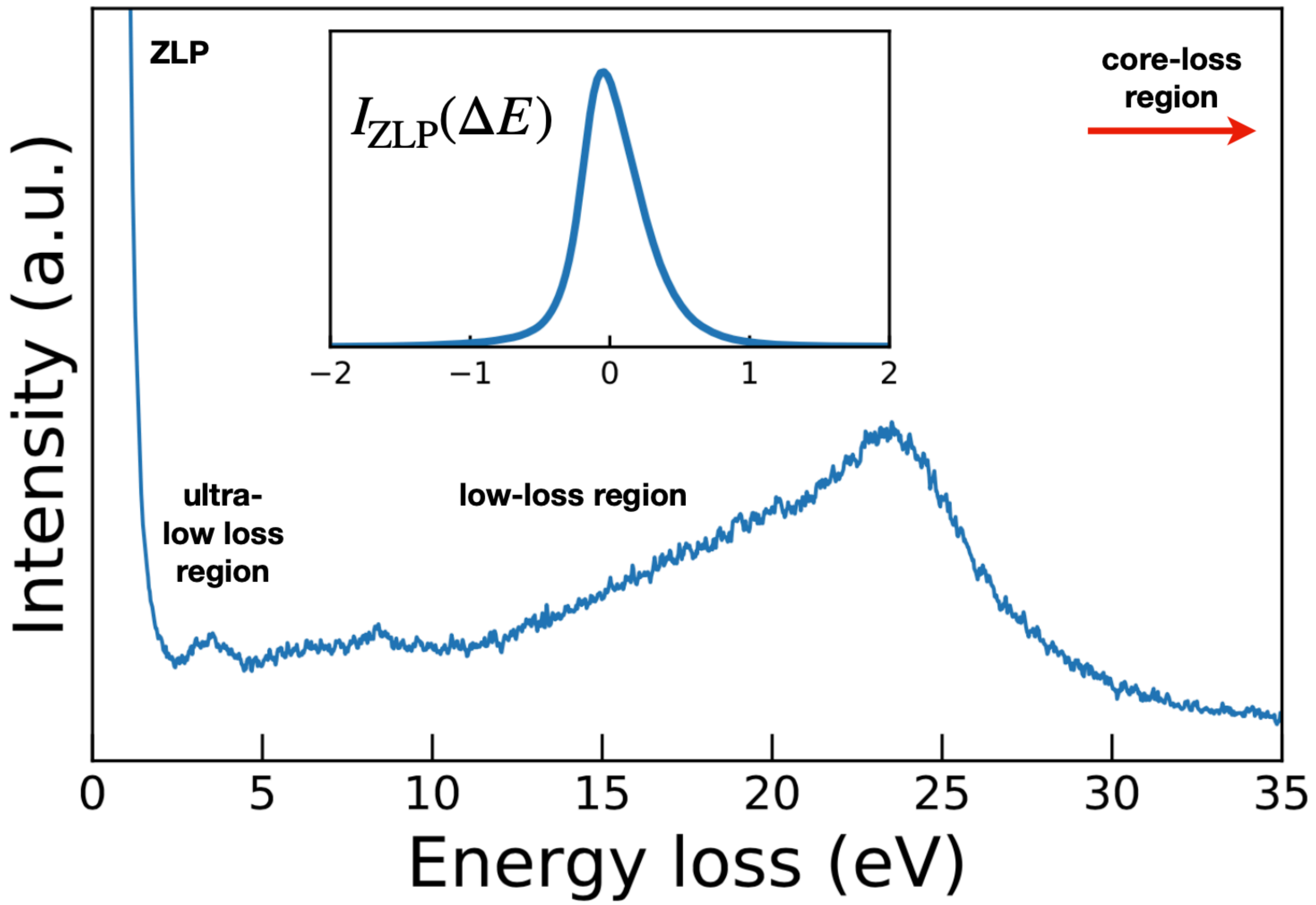

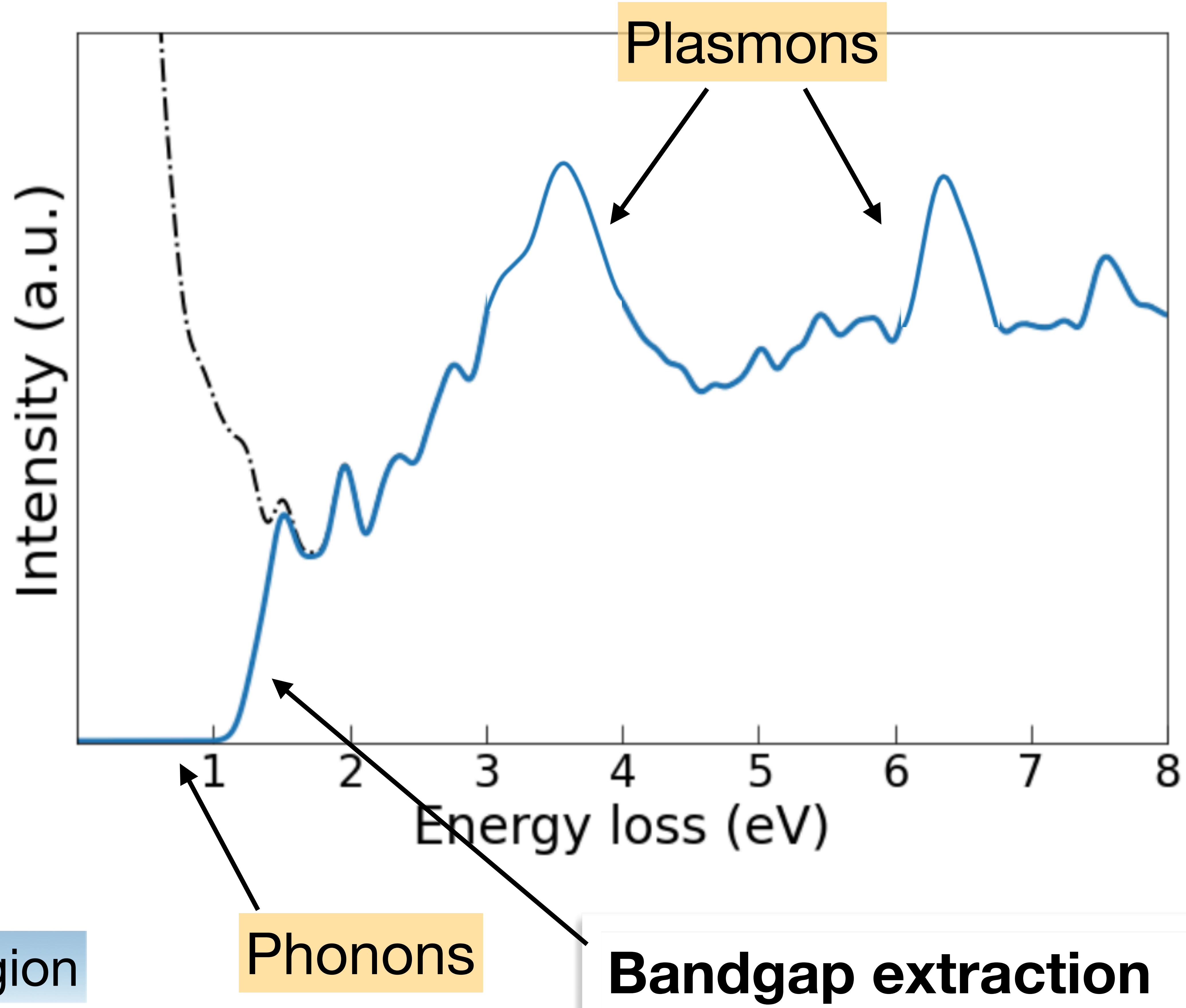

Bandgap extraction
From the onset of the inelastic spectrum

Zero-loss region

- Zero Loss Peak
- Elastically scattered electrons

Low-loss region

Inelastic interactions

- Plasmons
- Excitons
- Phonons

High-loss region

Ionisation edges

ZLP subtraction

Most general suggestion: subtraction of a fitted function

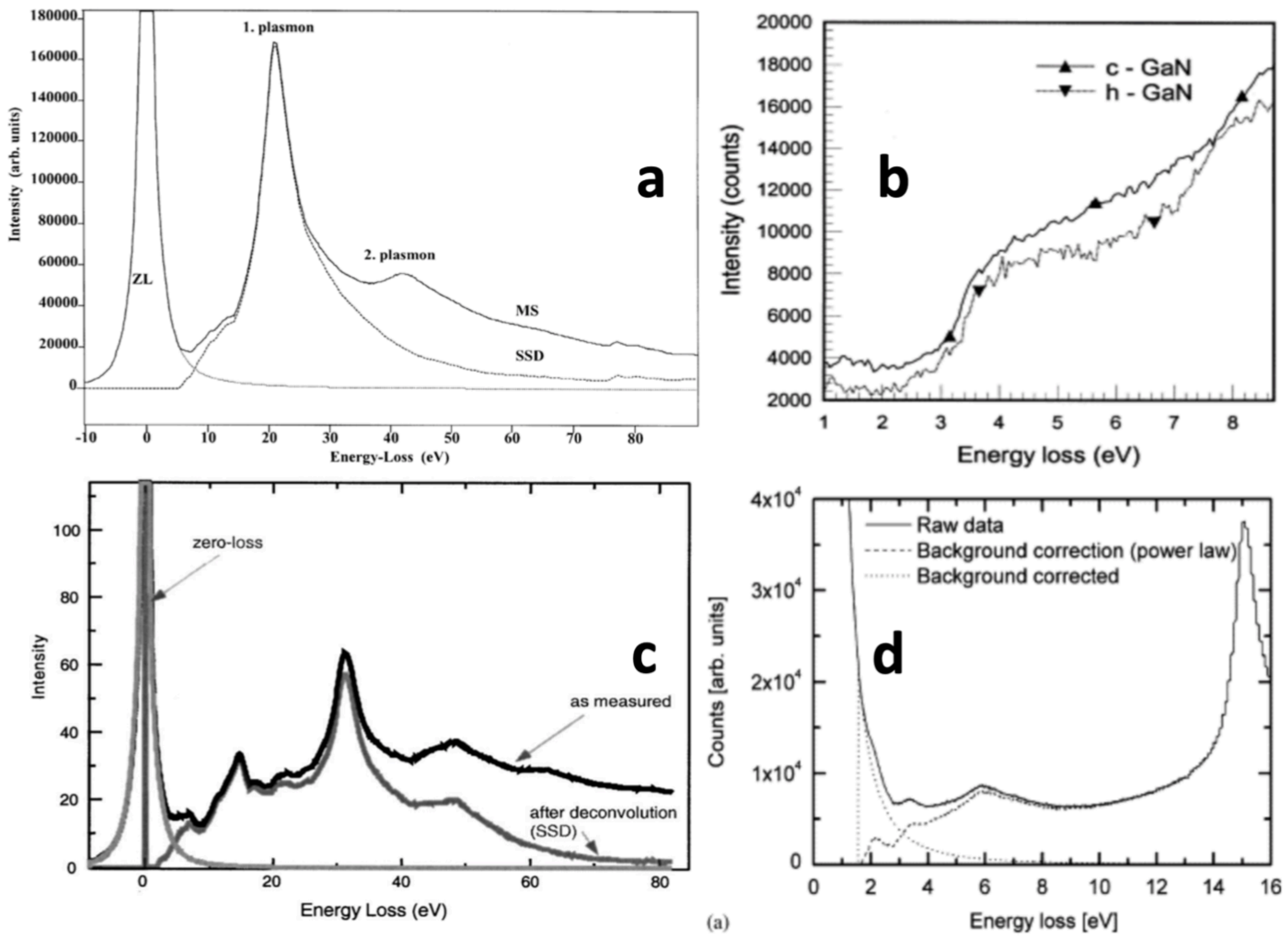

(a) Lorentzian [8]
(b) Mirroring left-hand side [9]
(c) Power-law [10]
(d) General multi-parameter [11]

General flaws:
- Model-dependent
- Based on assumptions
- No uncertainty estimate

Goal:
- Model-independent
- Unbiased
- Associated uncertainties

Artificial neural networks (ANN)

Neural networks provide a flexible, powerful method for many problems (forecasting, pattern recognition, classification, …)

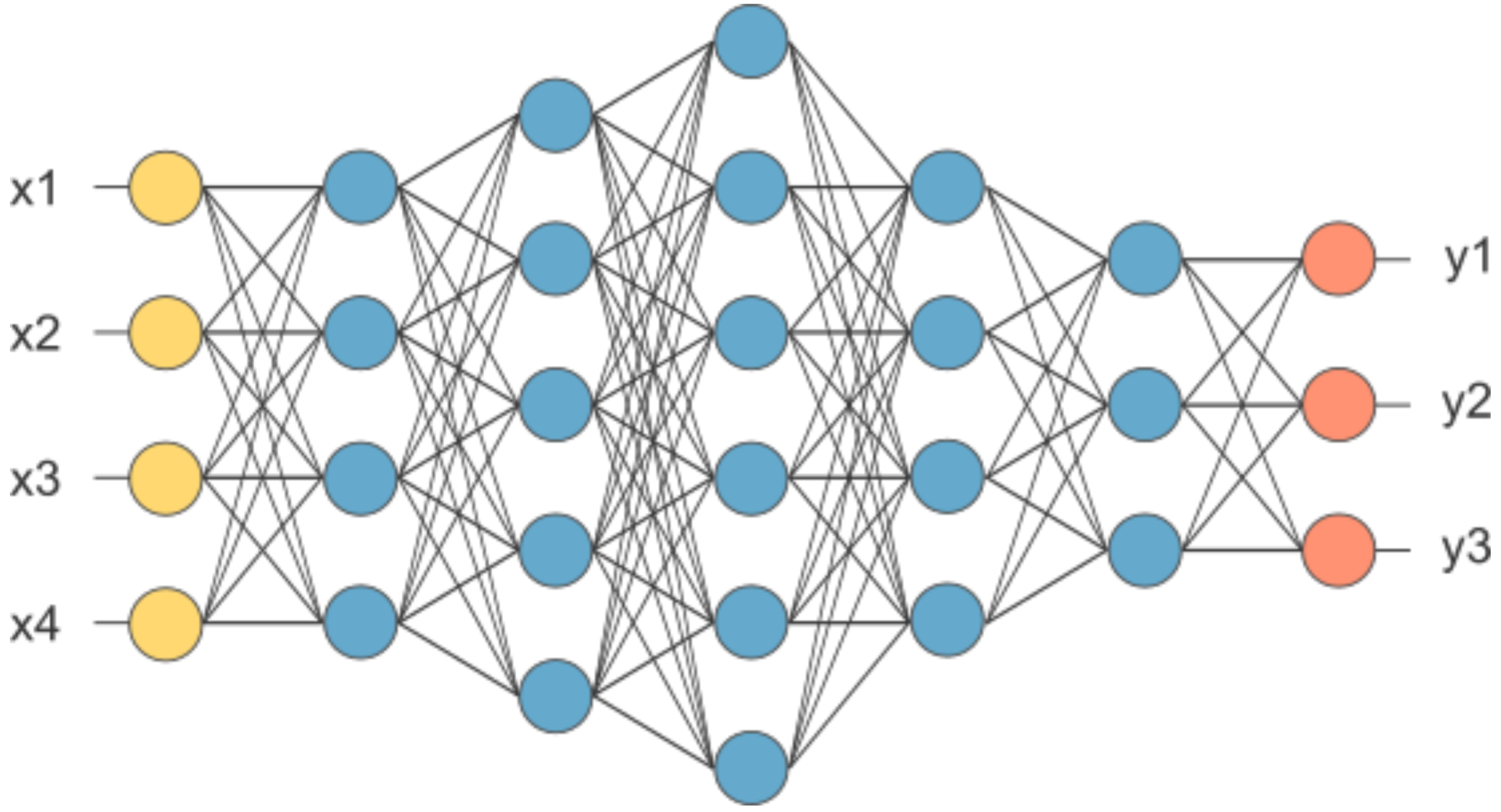

Supervised learning
Compare NN predictions with the target and use the **error** to tune the network parameters

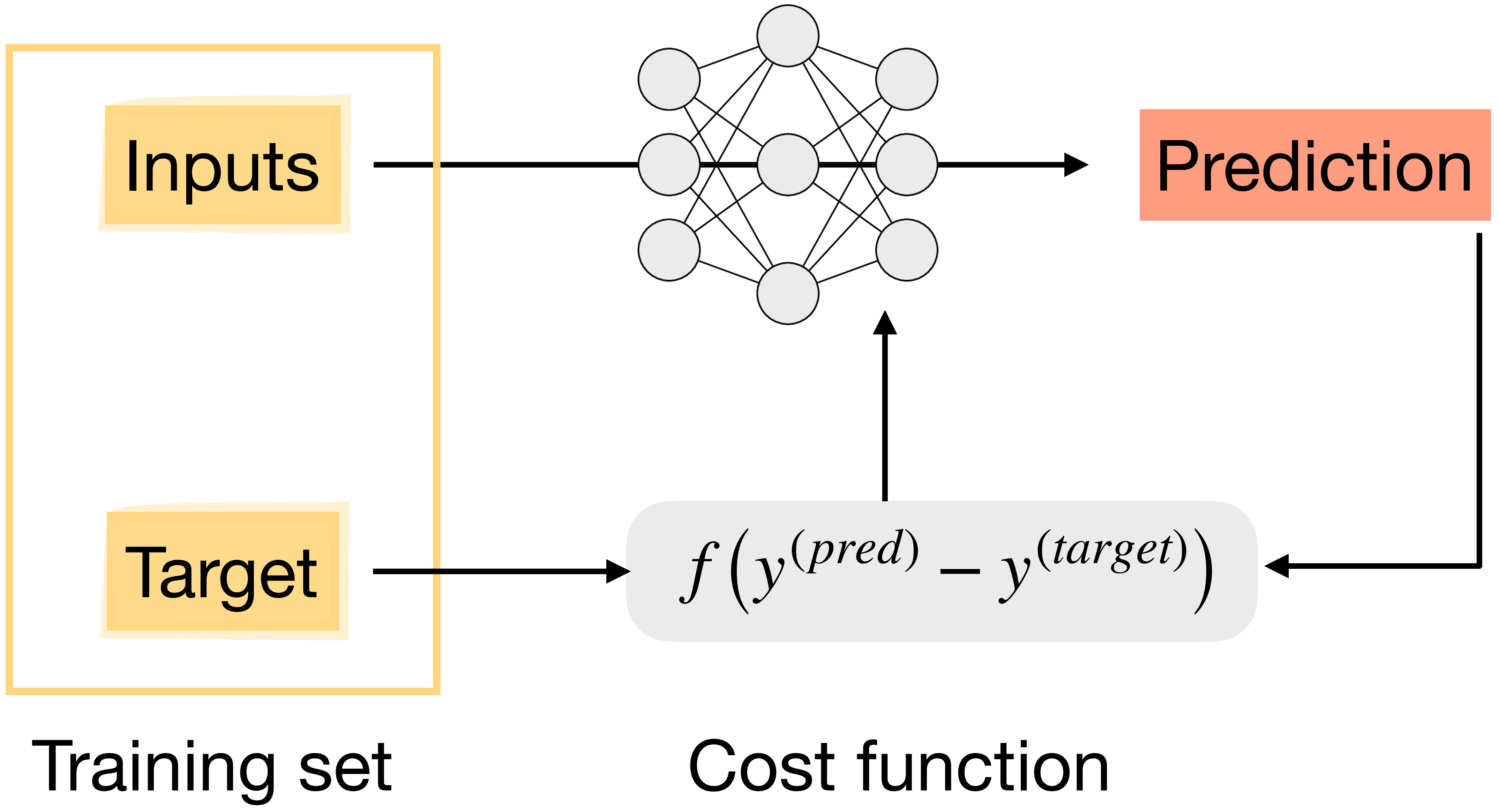

Optimal stopping

A neural network can **under-fit**, **over-fit** or **perfect-fit** the training data… So when to stop?

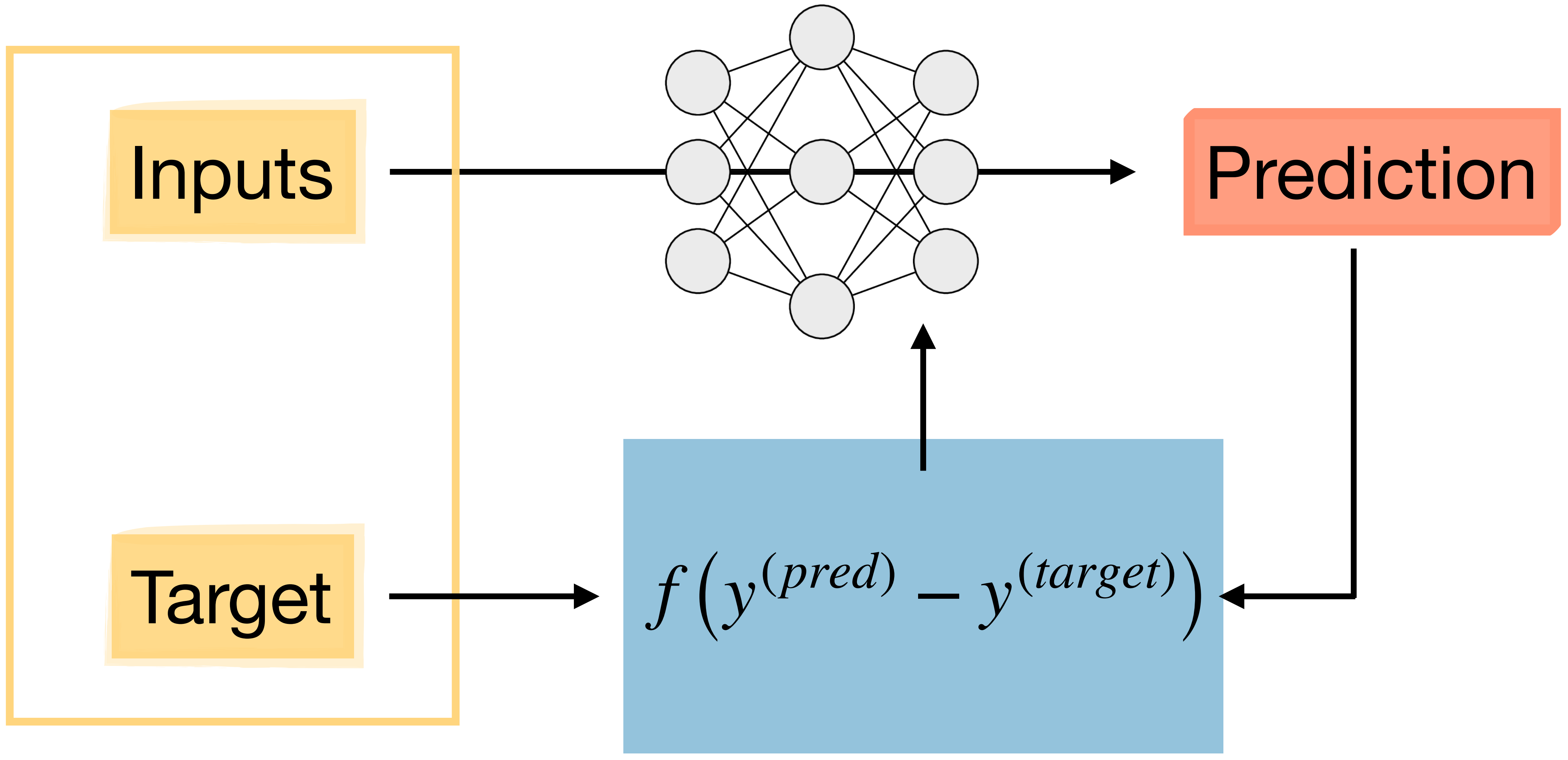

Training set

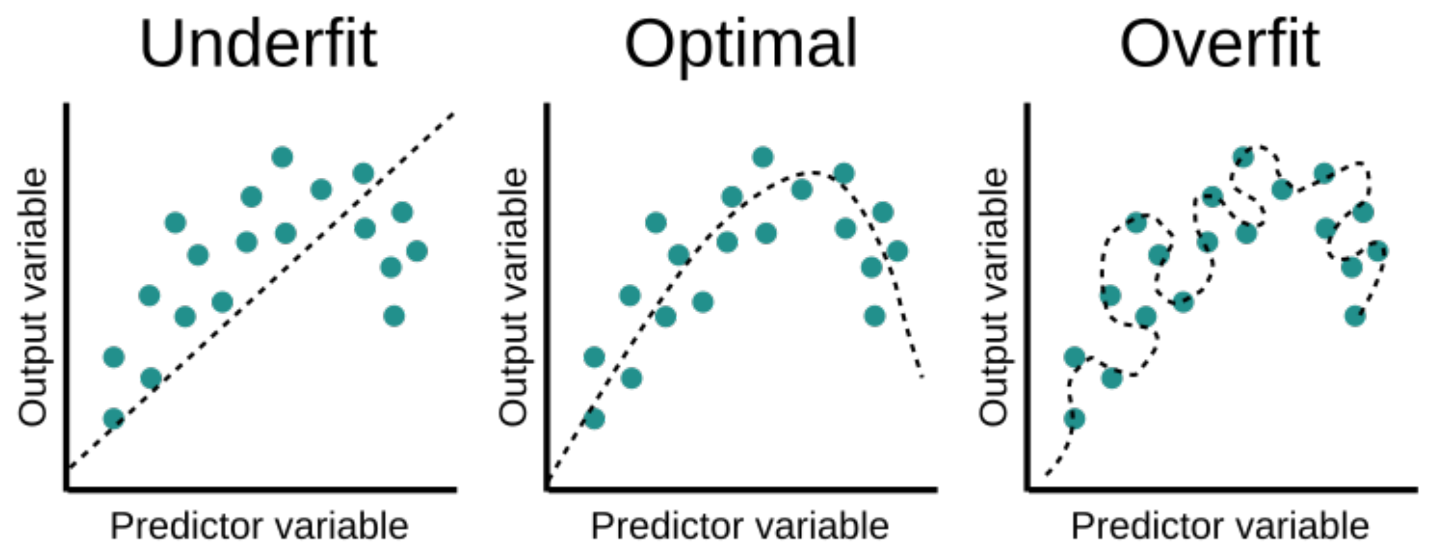

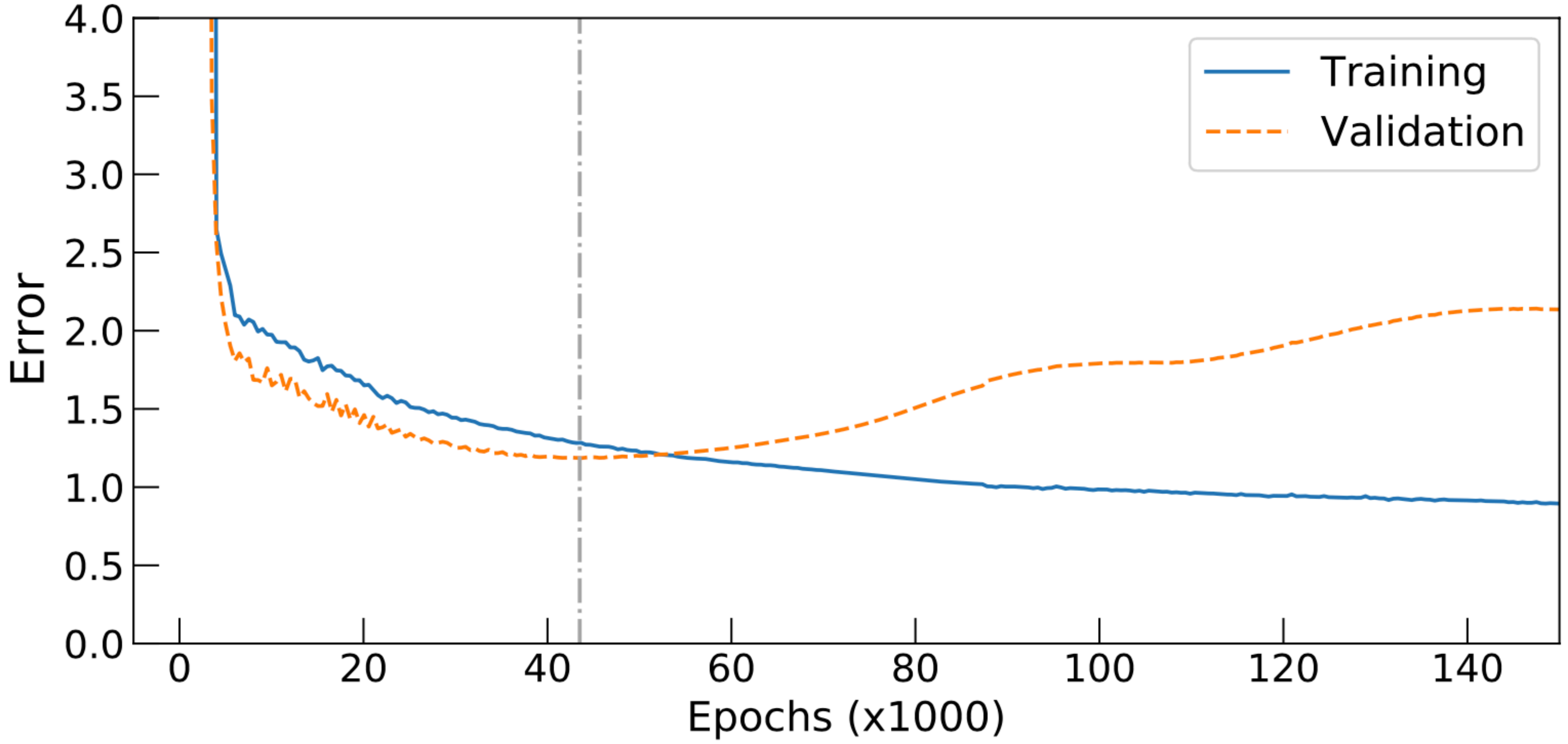

- Split the training set in **80%** training, **20%** validation
- Stop at the minimum validation error

Parametrization of the ZLP

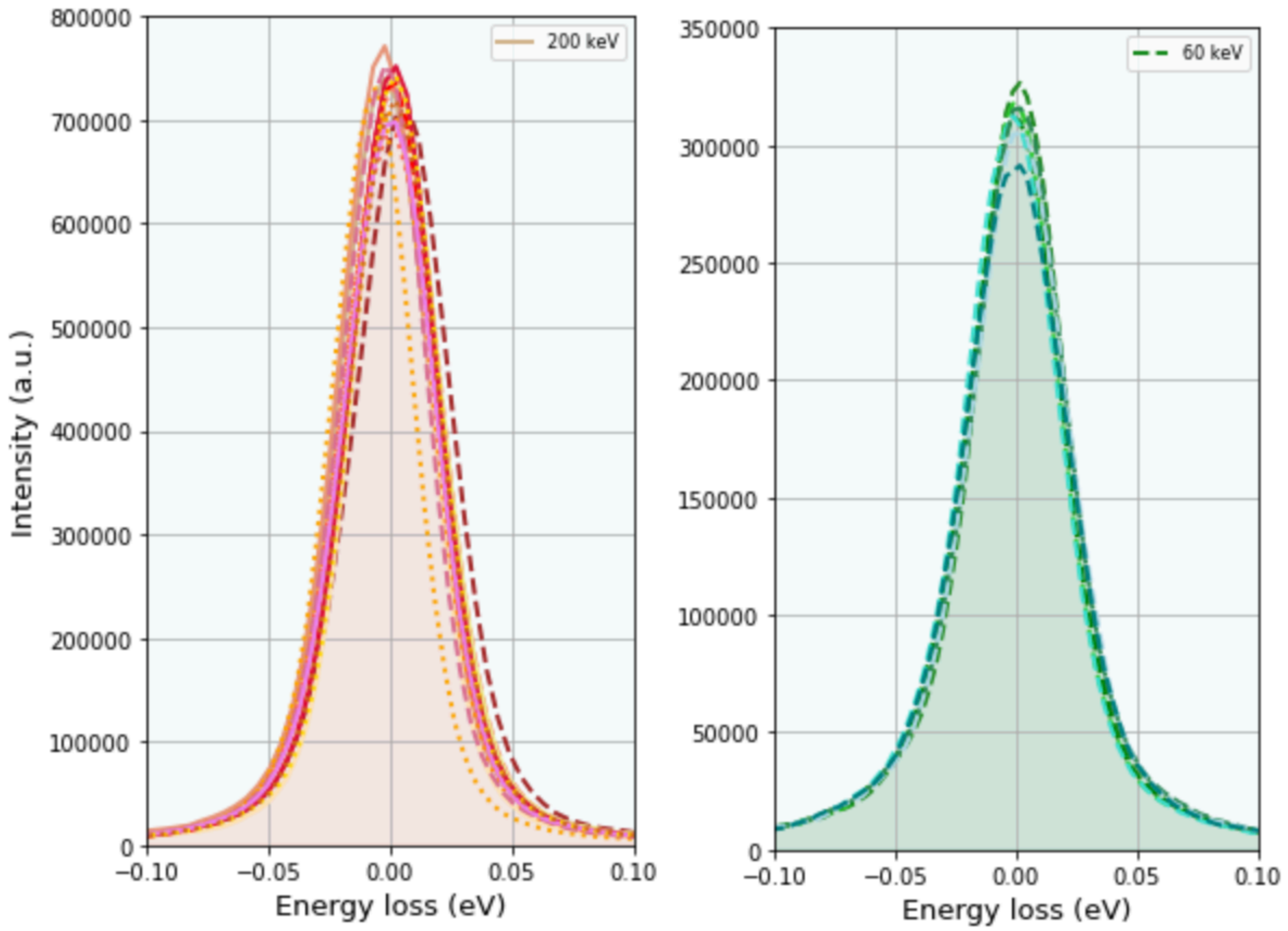

Inputs $\{\Delta E, t_{\text{exp}}, E_b\}$

- Energy loss
- Exposure time
- Beam energy

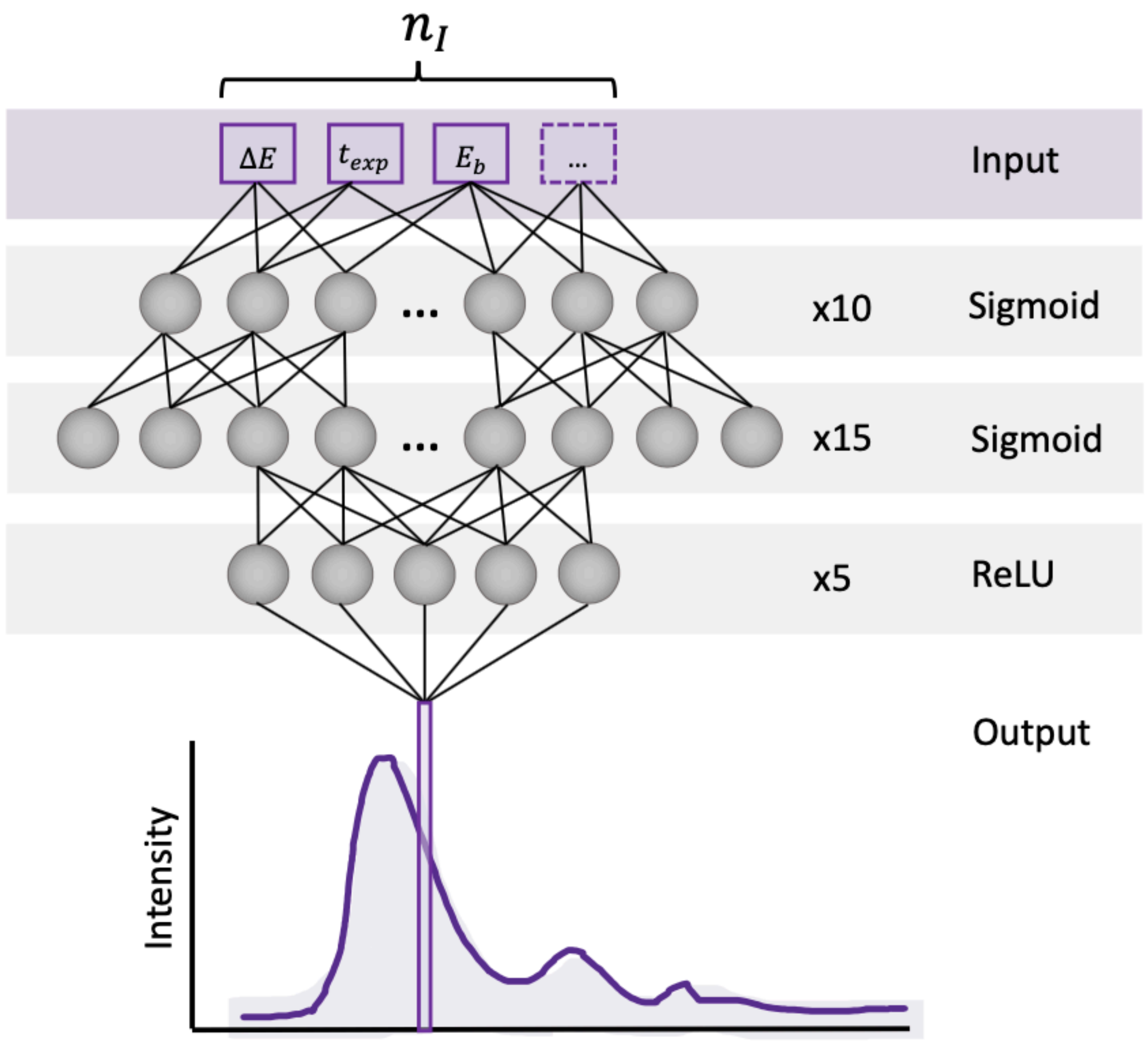

Target I_{ZLP}

- ZLP intensity

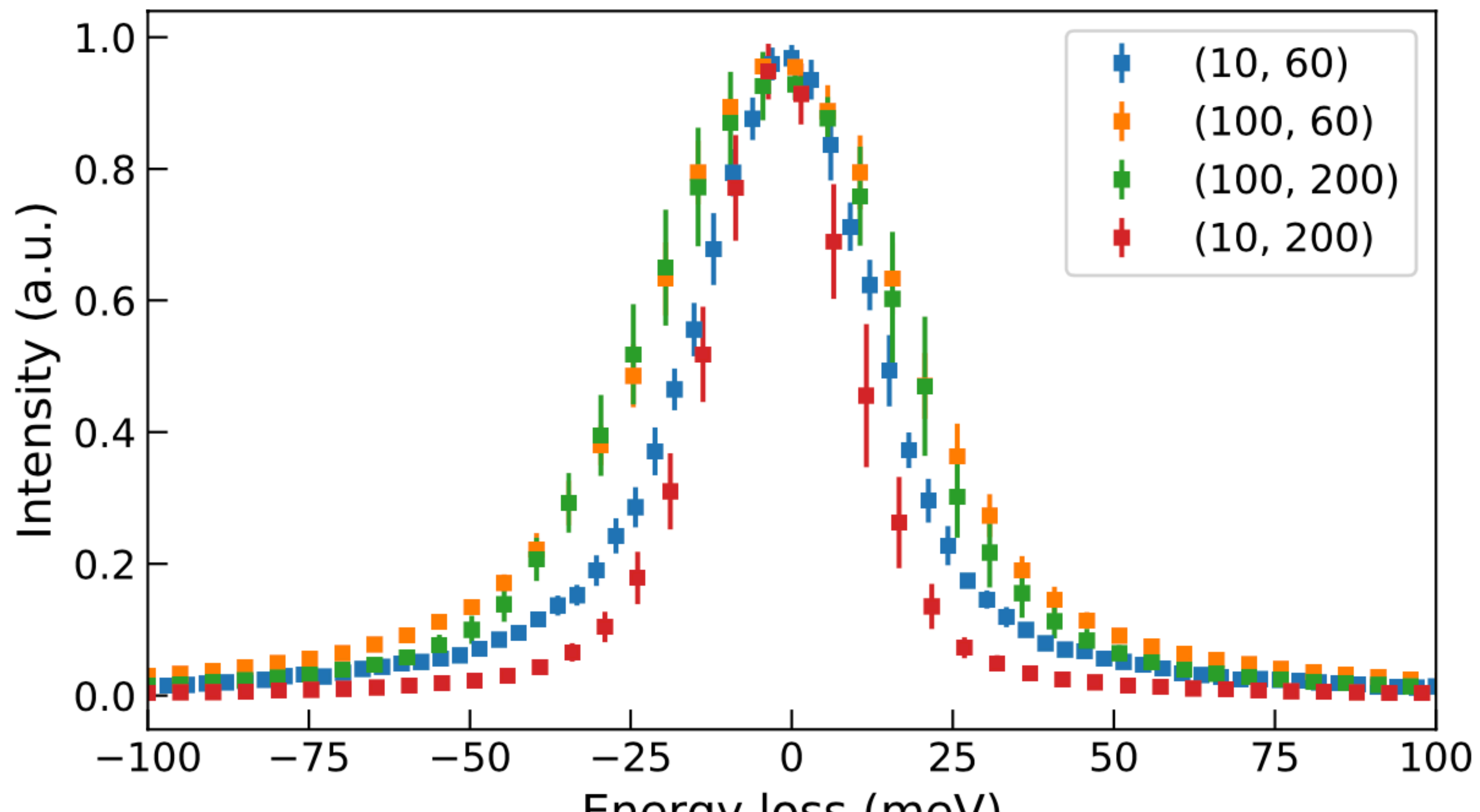

Motivation for training on vacuum peaks:

- Multidimensionality
- Flexibility
- Baseline for sample spectra

Training on sample spectra

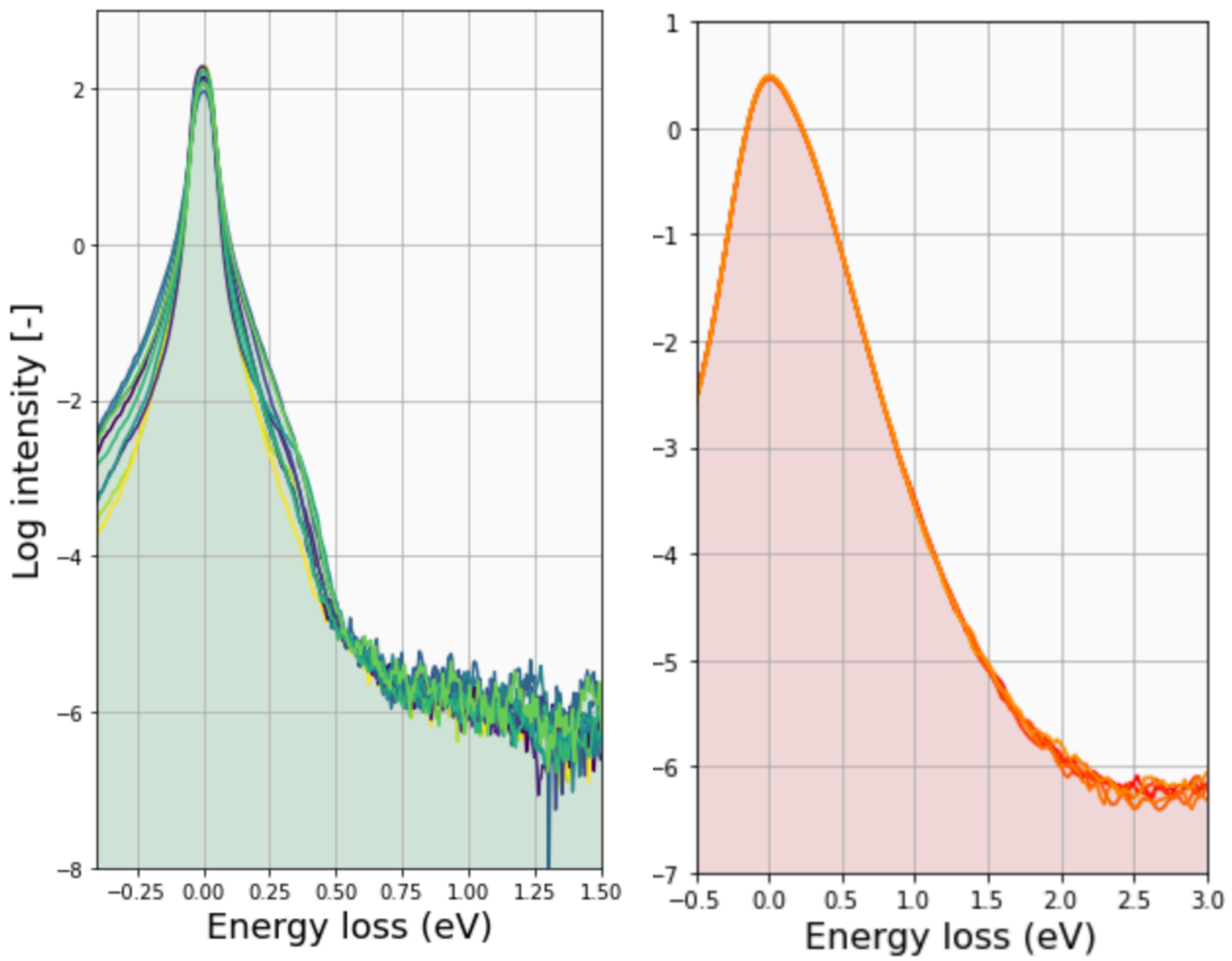

Inputs → Target

Energy loss $\{\Delta E\}$ ZLP intensity I_{ZLP}

$$I_{EEL}(\Delta E) = I_{ZLP}(\Delta E) + I_{inel}(\Delta E)$$

$$I_{\rm inel}(\Delta E) \simeq I_{EEL}(\Delta E) - I_{ZLP}^{(mod)}(\Delta E)$$

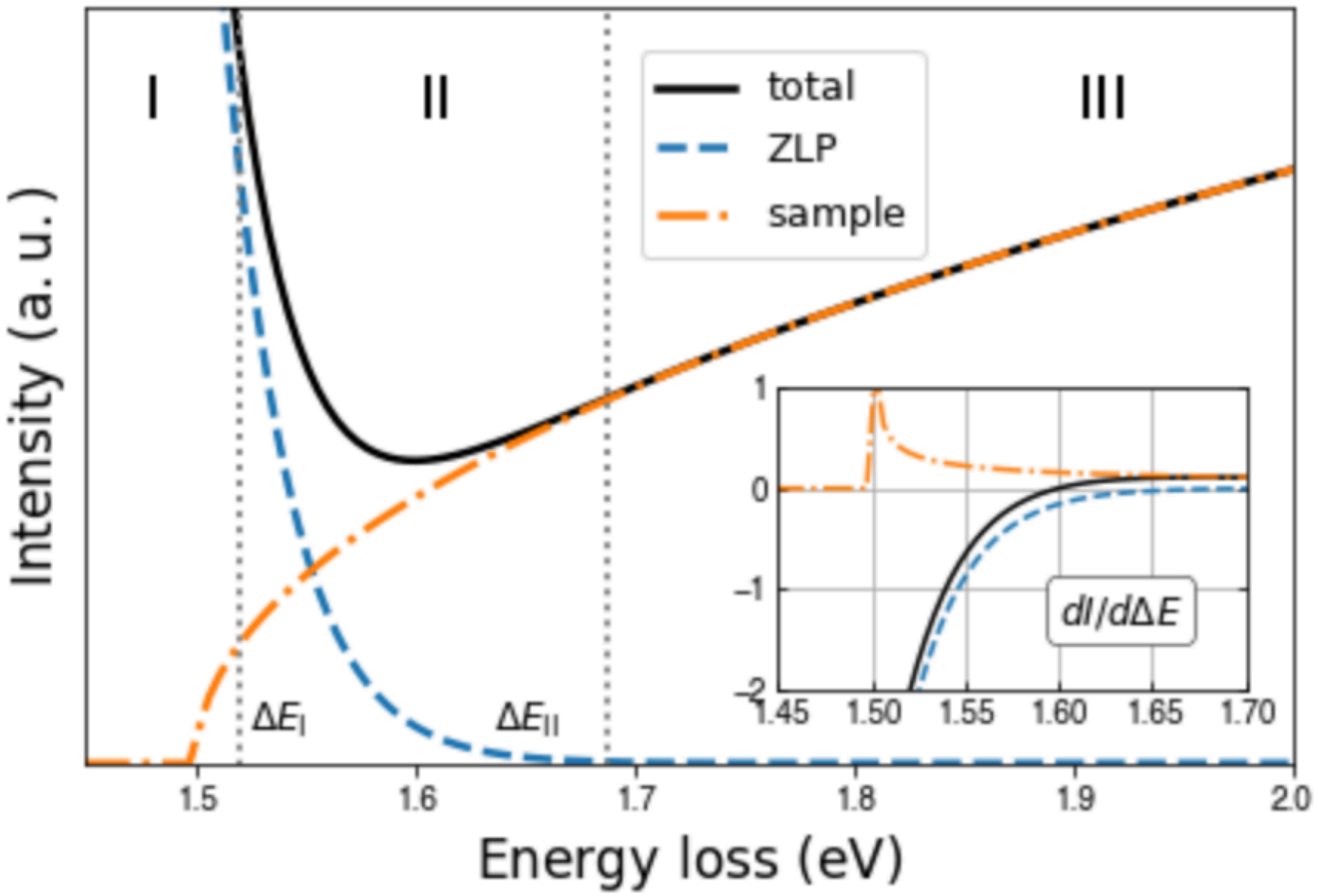

Region I. $(\Delta E < \Delta E_I)$
ZLP-regime: keep training data

Region II. $(\Delta E_I < \Delta E < \Delta E_{II})$
Interpolation regime: drop training data

Region III. $(\Delta E > \Delta E_{II})$
ZLP intensity goes to zero → add pseudo data

Uncertainty propagation

Goal:
- Model-independent
- Unbiased
- **Associated uncertainties**

Monte Carlo replica method

$$\sigma^{(mod)}_{I_{ZLP}} = \left(\frac{1}{N_{rep}-1} \sum_{k=1}^{N_{rep}} \left(I^{(mod)(k)}_{ZLP} - \left\langle I^{(mod)}_{ZLP} \right\rangle \right) \right)^{1/2}$$

$$\left\langle I^{(mod)}_{ZLP} \right\rangle = \frac{1}{N_{rep}} \sum_{k=1}^{N_{rep}} I^{(mod)(k)}_{ZLP}$$

MC replicas
Artificial data

$$I^{(art)(k)}_{ZLP} = I^{(exp)}_{ZL} + r^{(k)}_i \sigma^{(exp)}_i$$

Predictions

Experimental data
- Central values
- Uncertainties

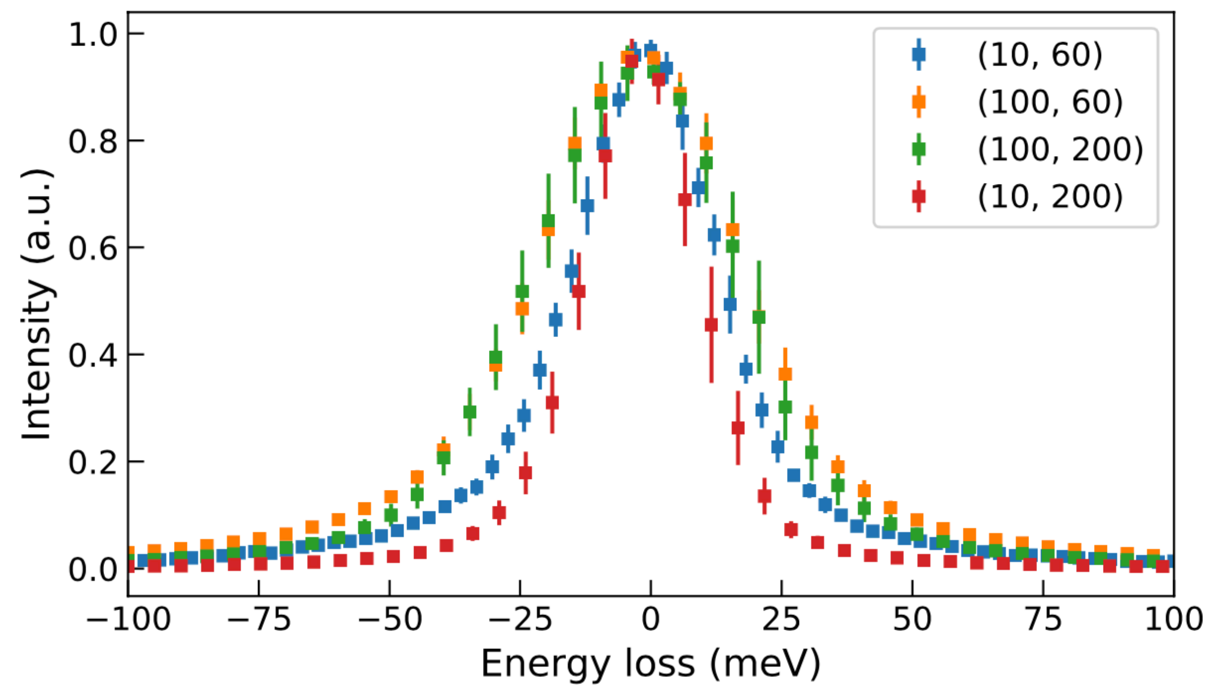

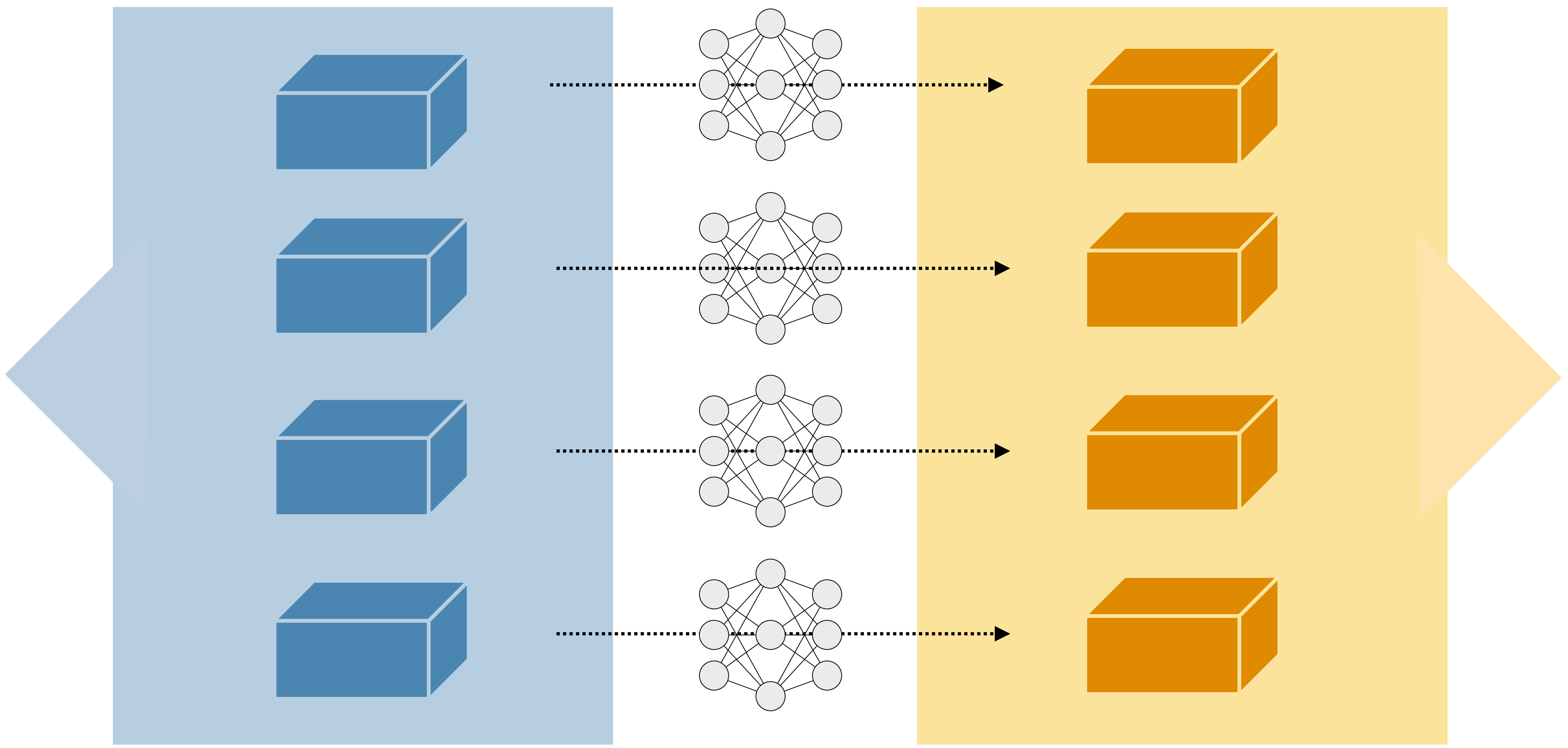

MC ensemble
- Central values
- **Uncertainties**

$$k = 1,2,\ldots,N_{rep} = 500$$

Computation time:
~ 20s/replica

Results part I - Vacuum spectra

Fit quality

$$\chi^2 = \frac{1}{n_{dat}} \sum_{i=1}^{n_{dat}} \left(\frac{I^{(exp)}_{ZLP,i} - I^{(mod)(k)}_{ZLP,i}}{\sigma_i^{(exp)}} \right)$$

Chi-square is a measure for how well the model describes the data

- $\chi^2 \simeq 1$ means satisfactory results

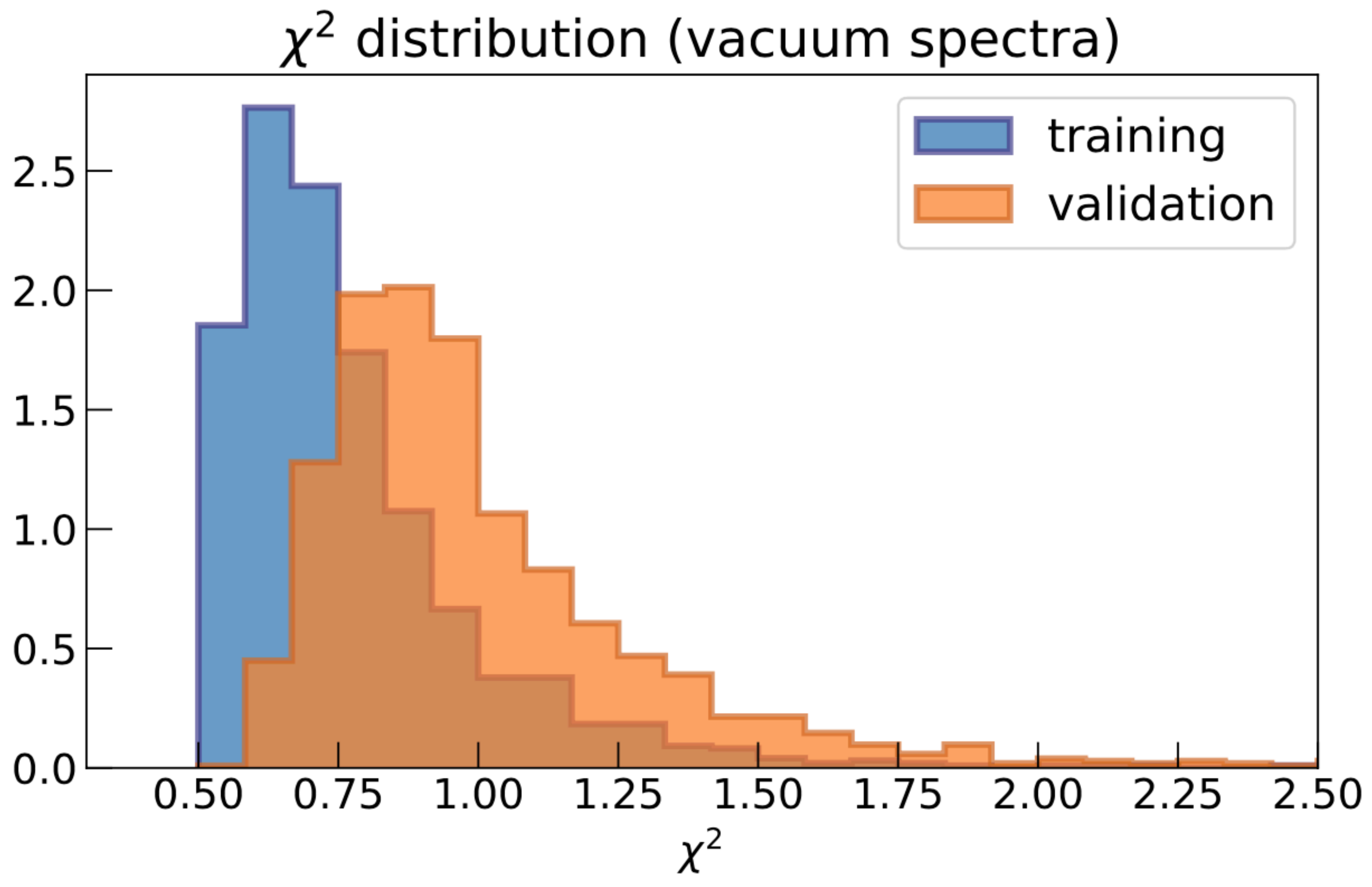

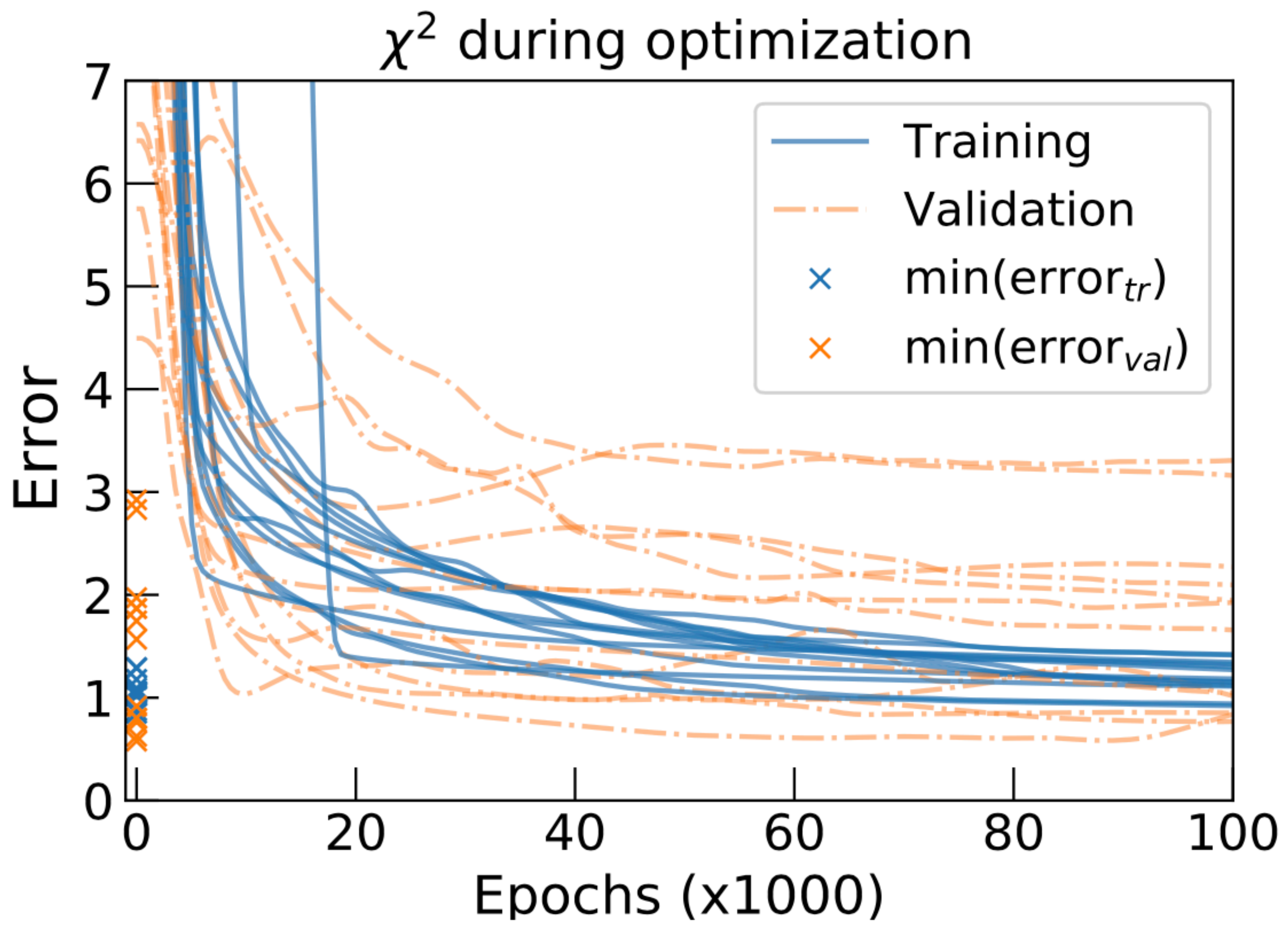

Results part I - Vacuum spectra

Dependence on energy loss (ΔE)

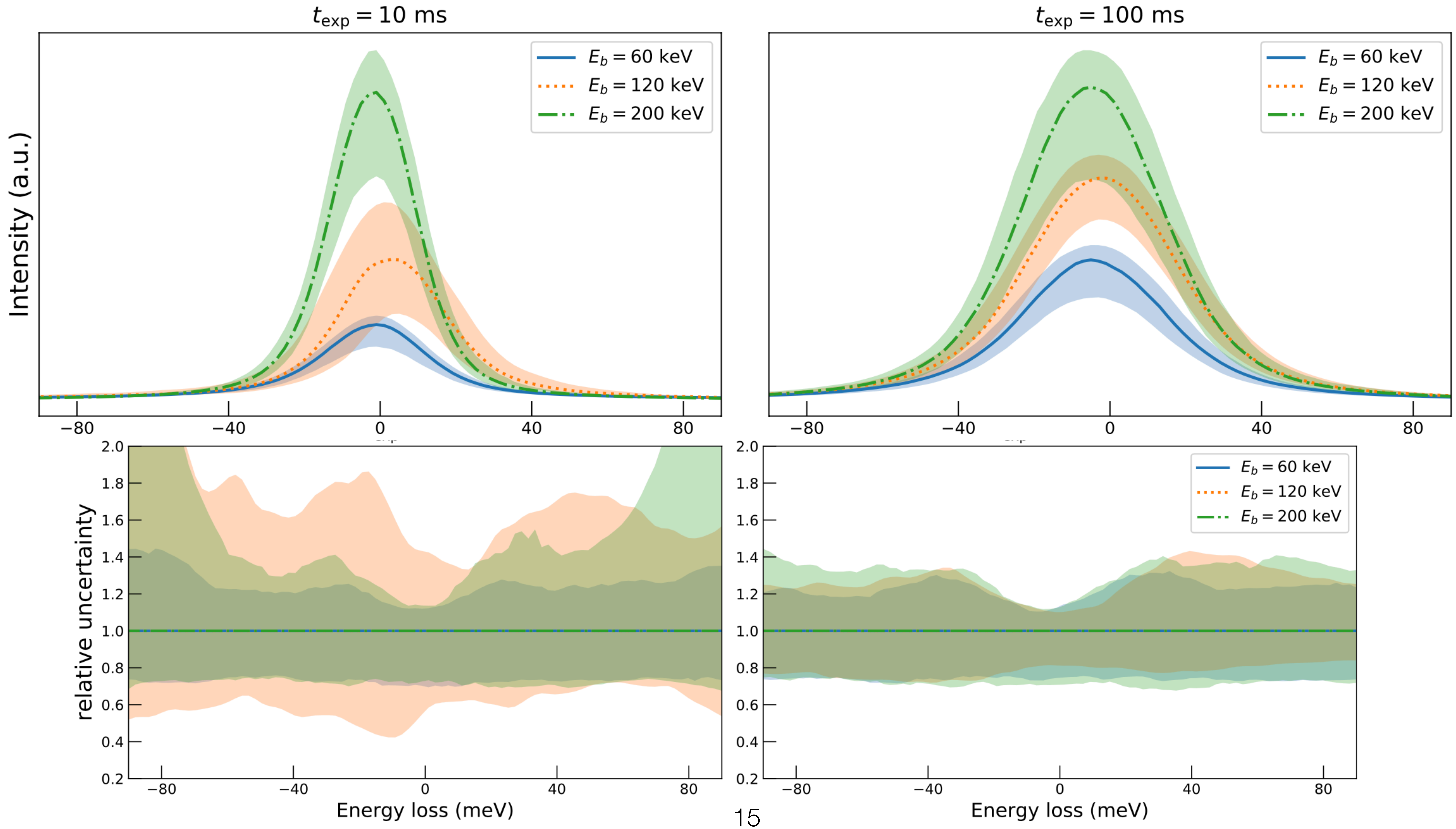

Results part I - Vacuum spectra

Dependence on E_b and t_{exp}

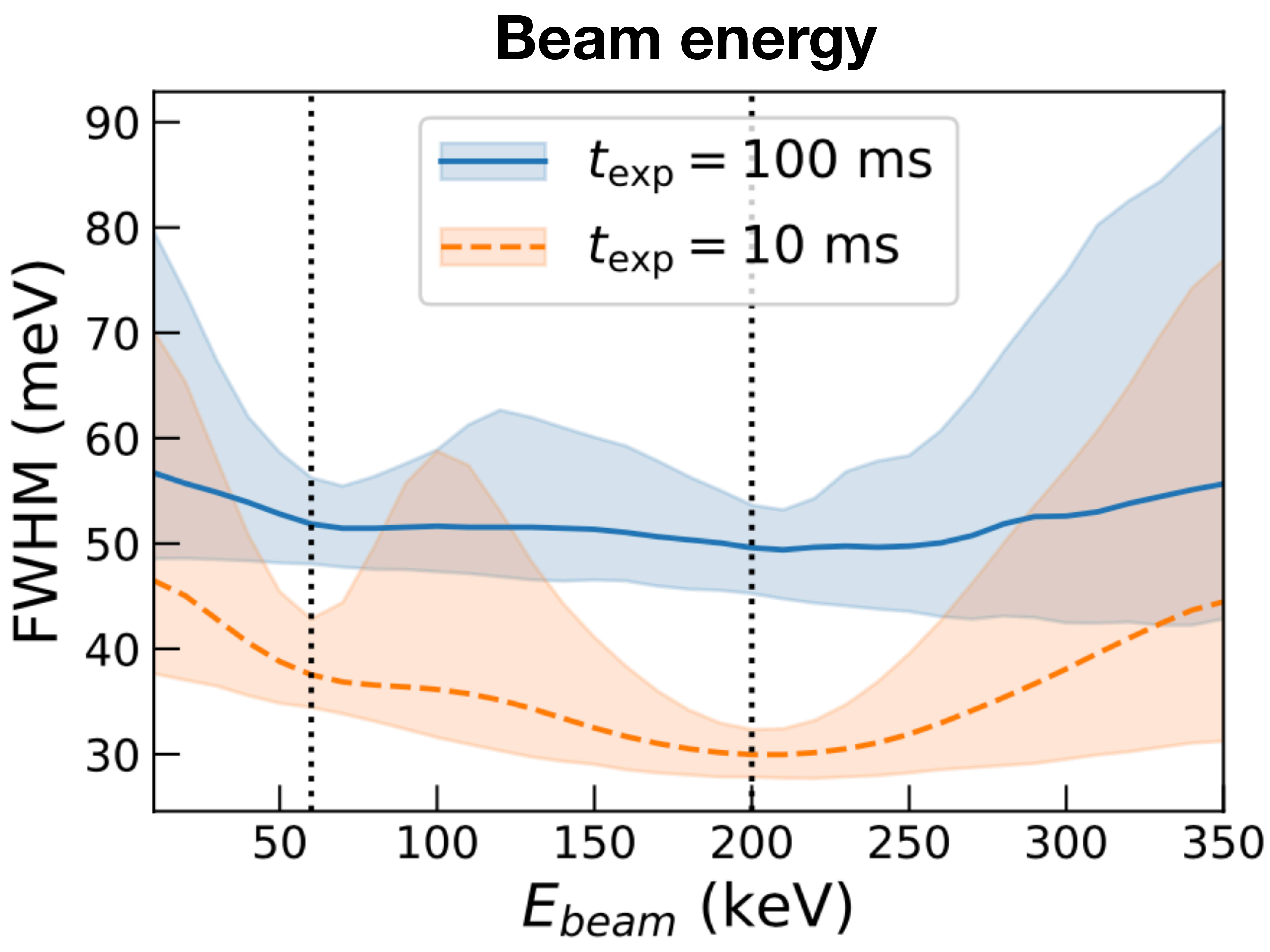

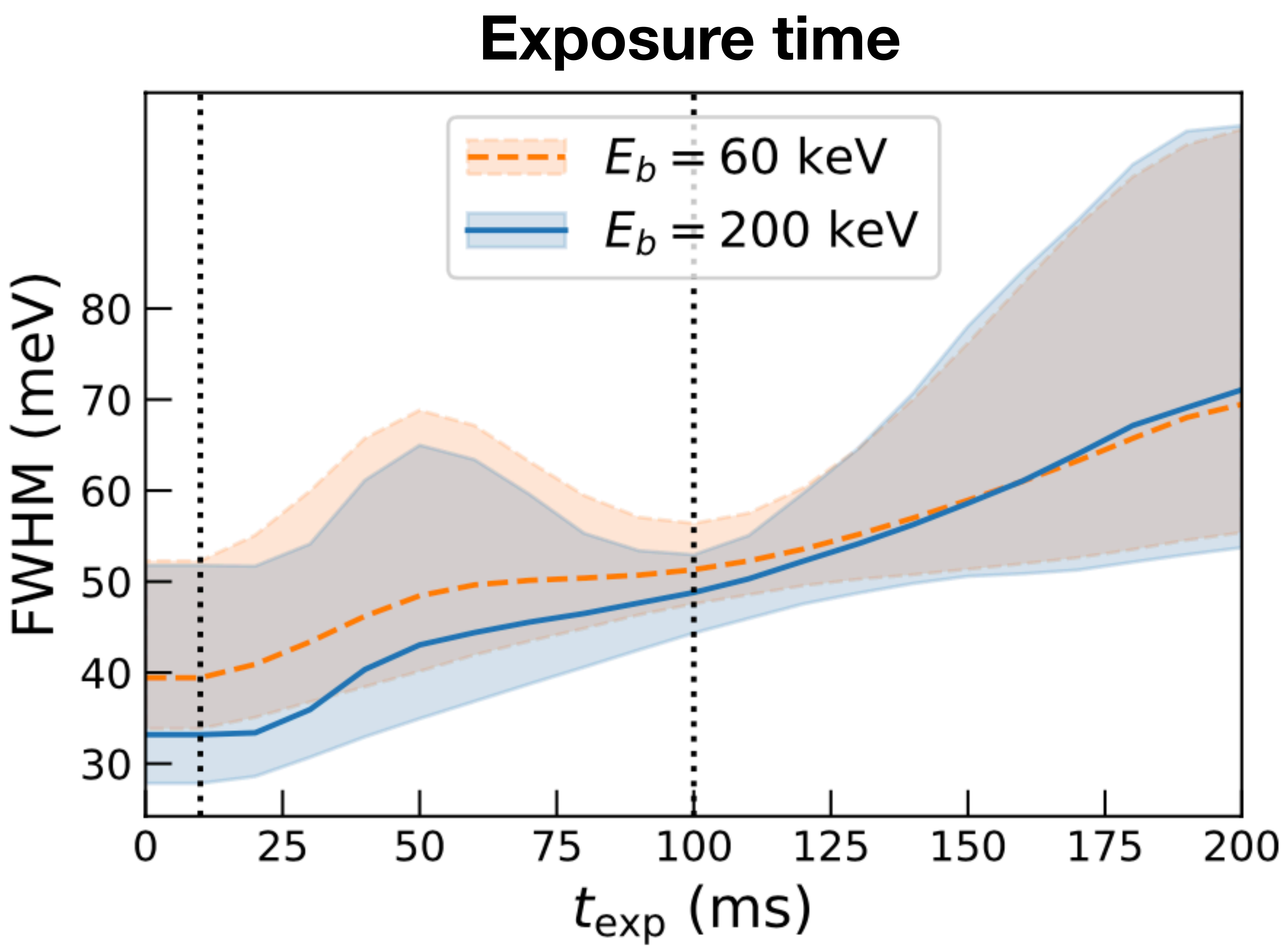

Results part I - Vacuum spectra

Removing a subset of data

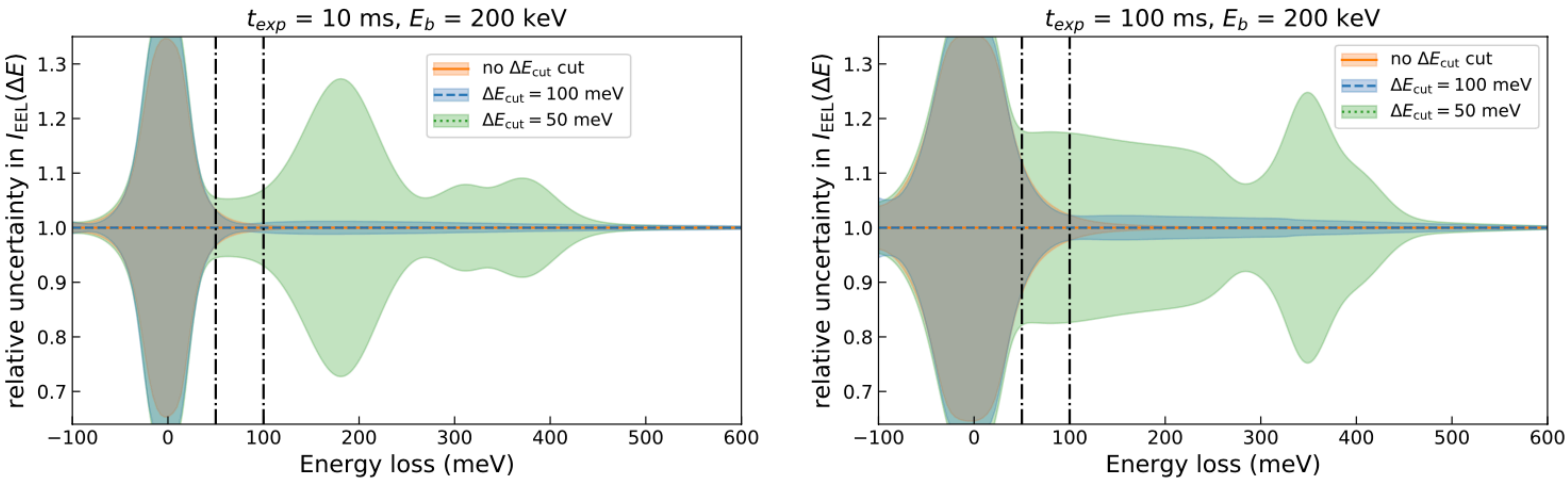

Results part II - Sample spectra

Tungsten disulfide (WS_2) nanoflowers

- TMD material
- Thickness dependent
- Polytypism

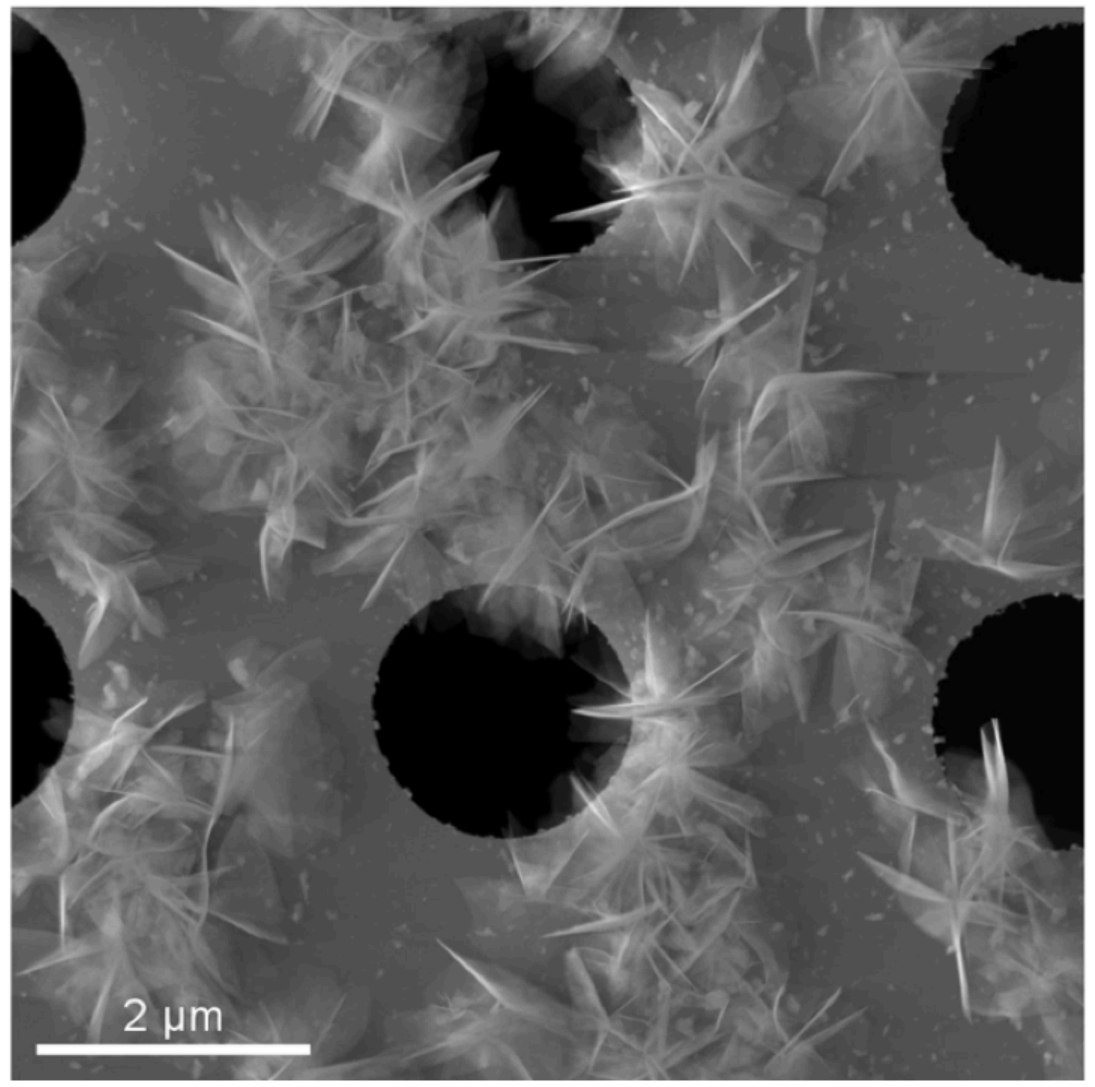

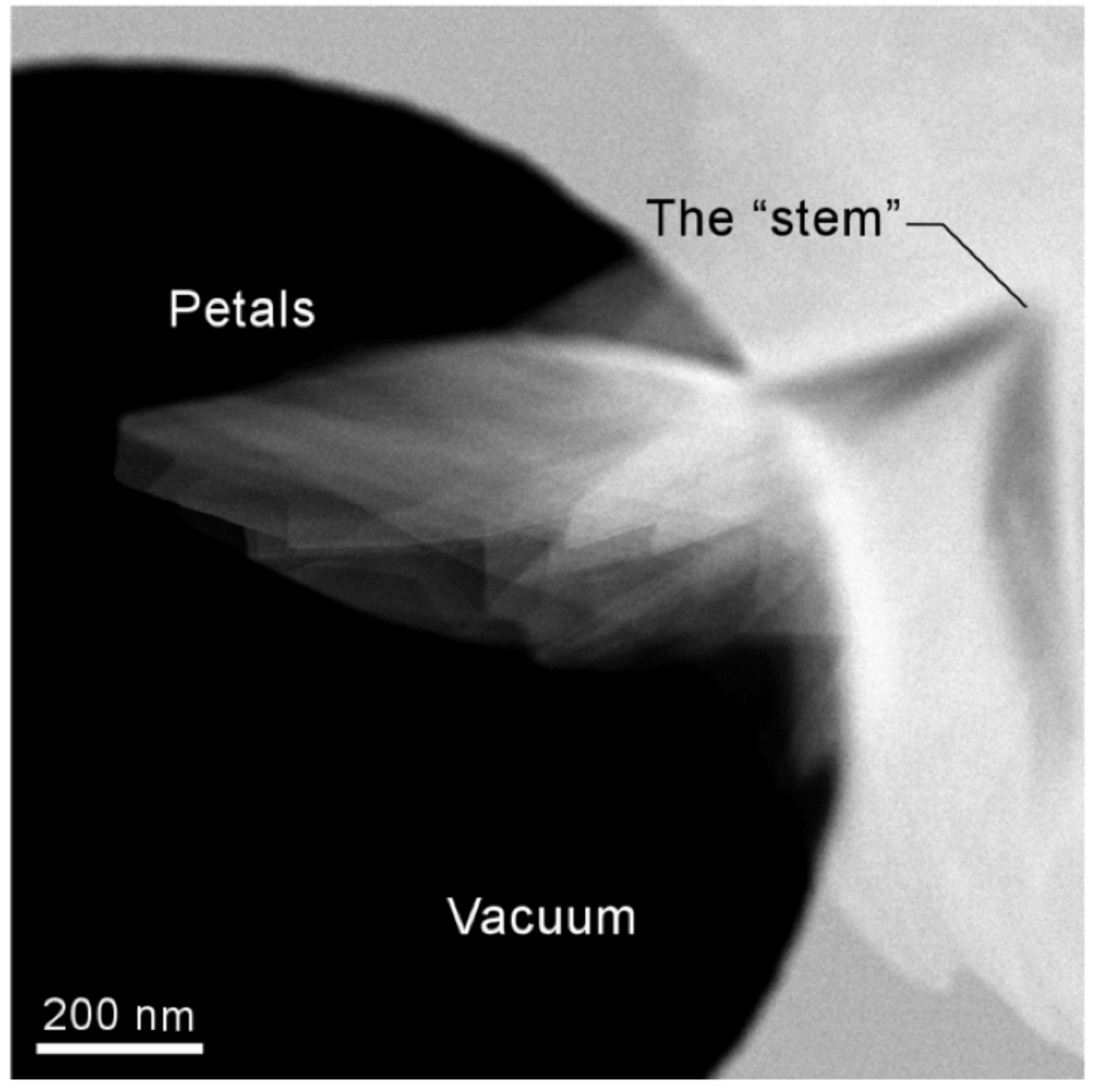

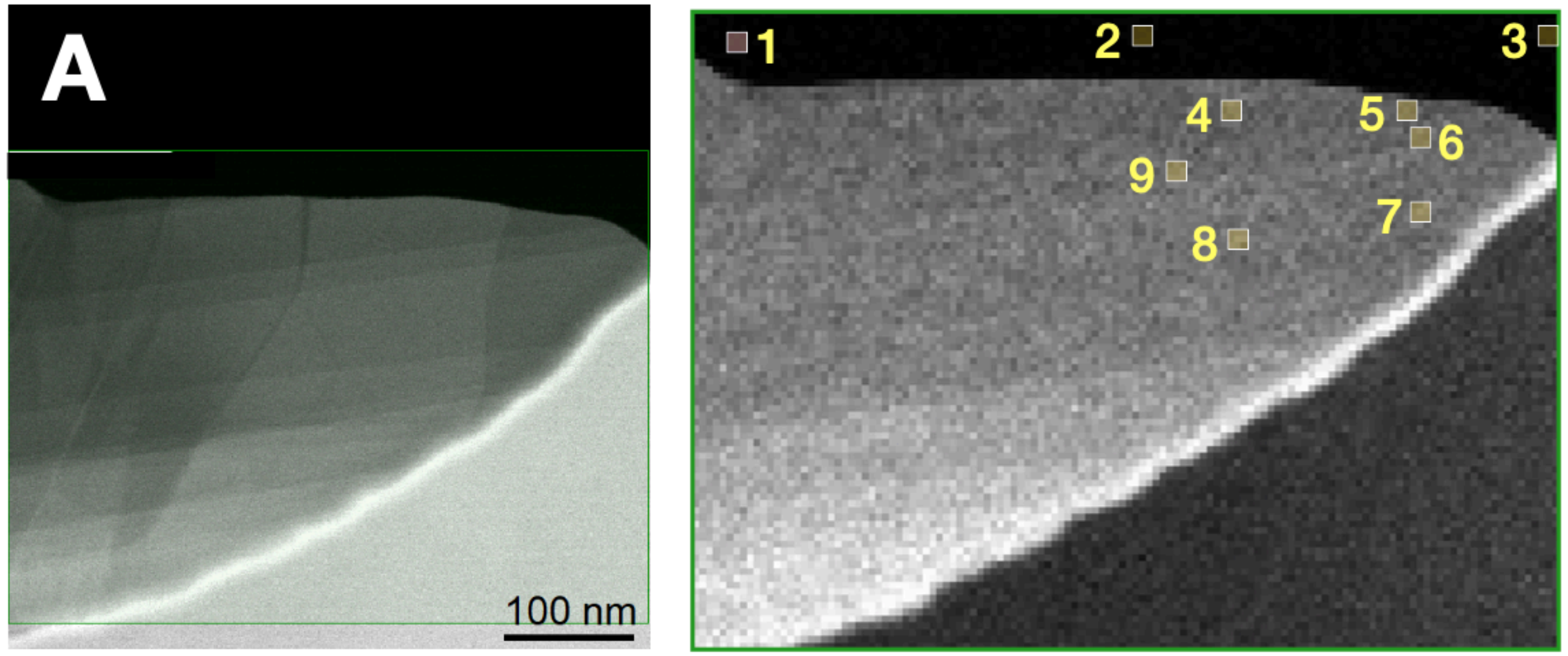

Sample A
Relatively thick
470 meV resolution

Sample B
Relatively thin
87 meV resolution

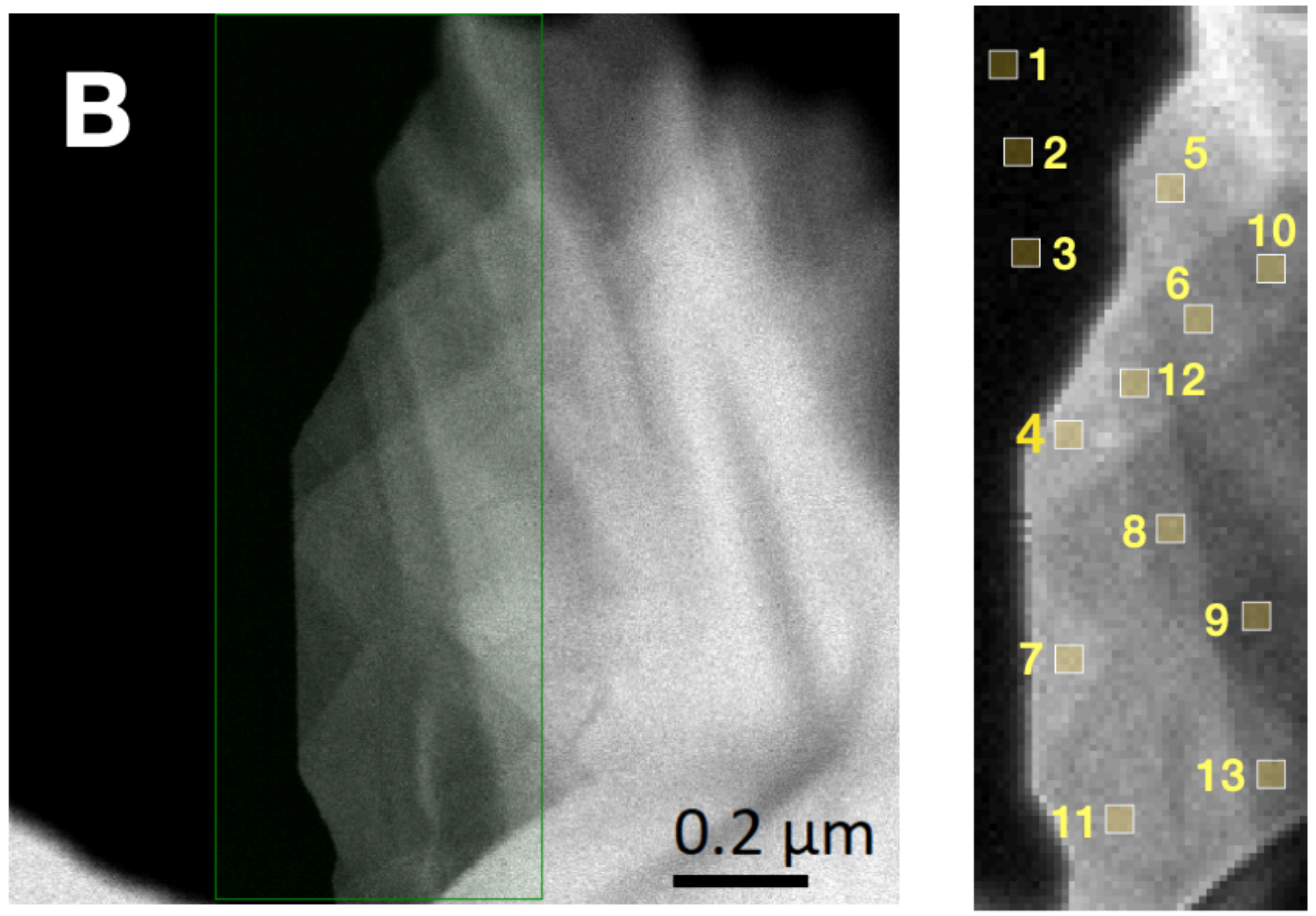

Results part II - Sample A

Predicted ZLP and subtracted spectrum

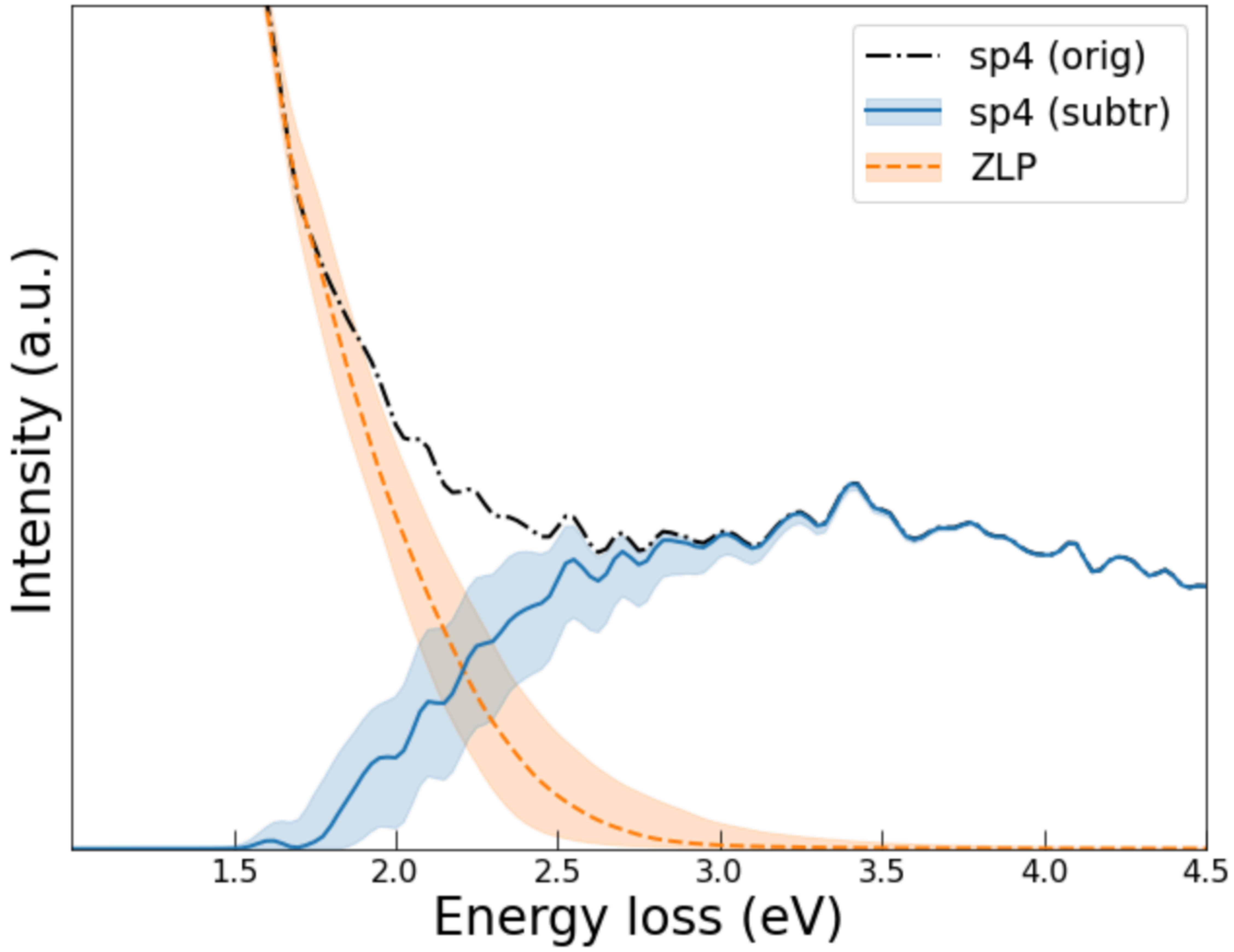

$$I_{inel} \propto (\Delta E - E_{BG})^b$$

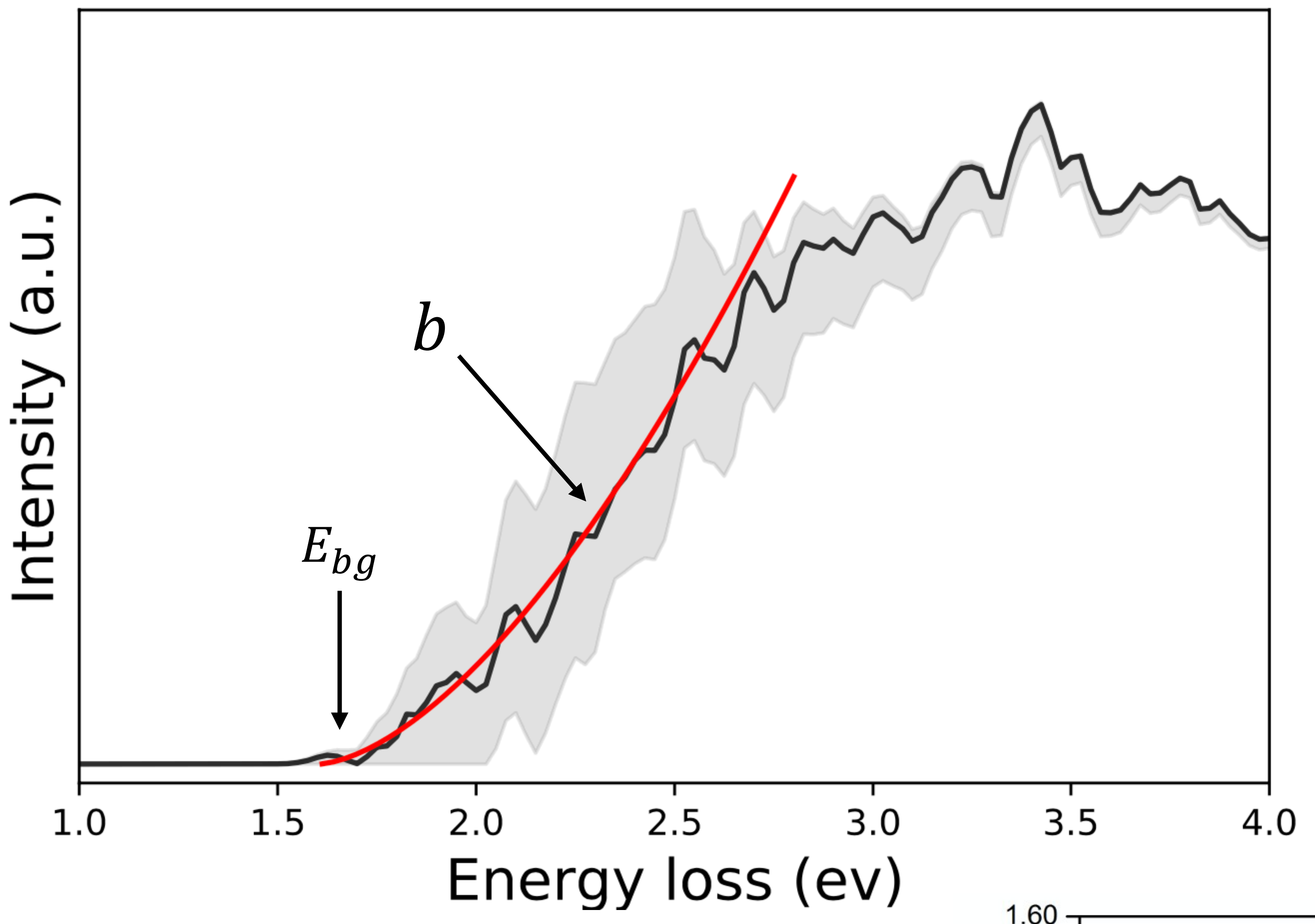

Bandgap
$b = 1/2$: direct
$b = 3/2$: indirect

$$E_{BG} = 1.6^{+0.3}_{-0.2} eV$$

$$b = 1.3^{+0.3}_{-0.7}$$

Theoretical DFT results, work in progress (Luigi)

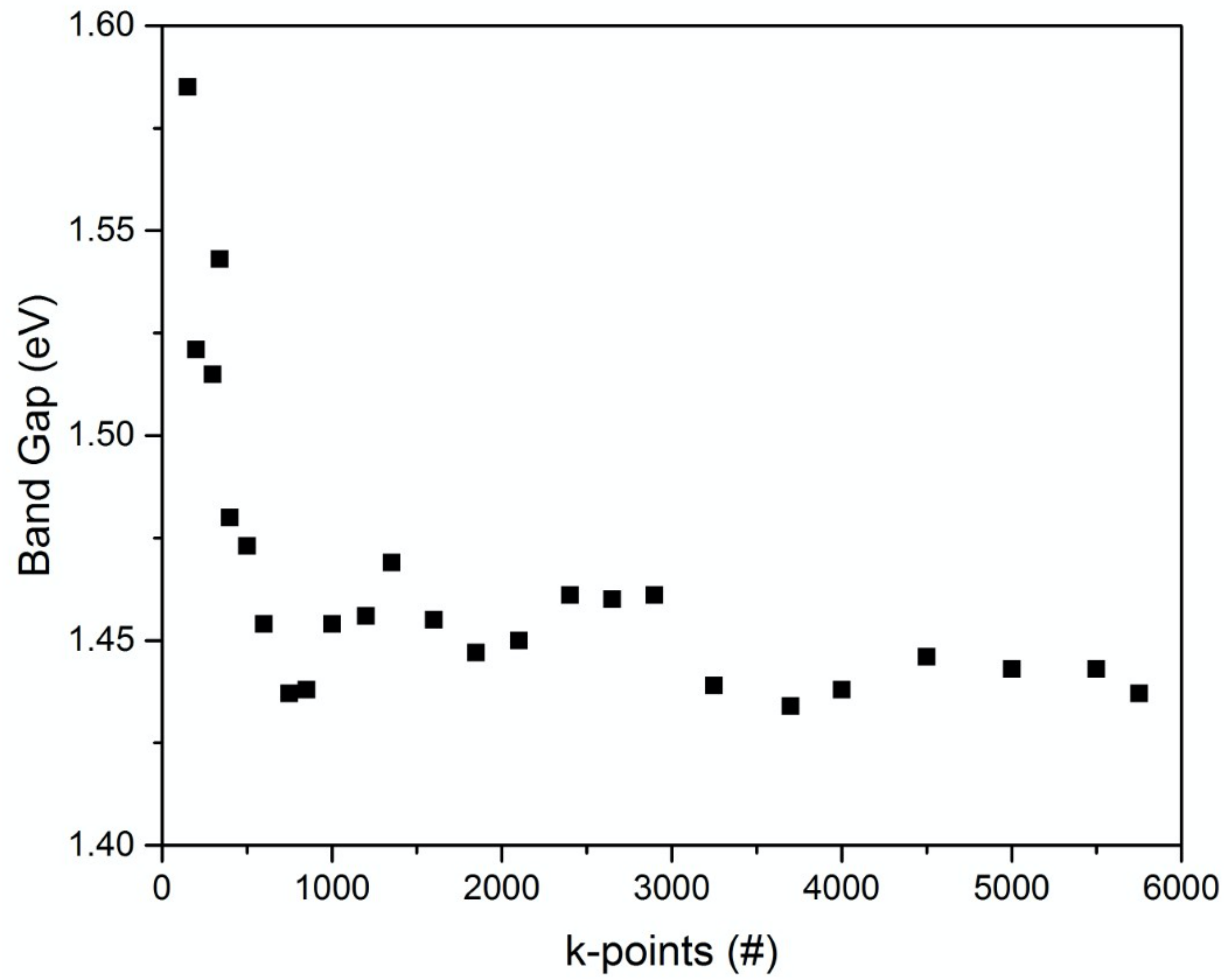

Results part II - Sample B

Predicted ZLP and subtracted spectrum

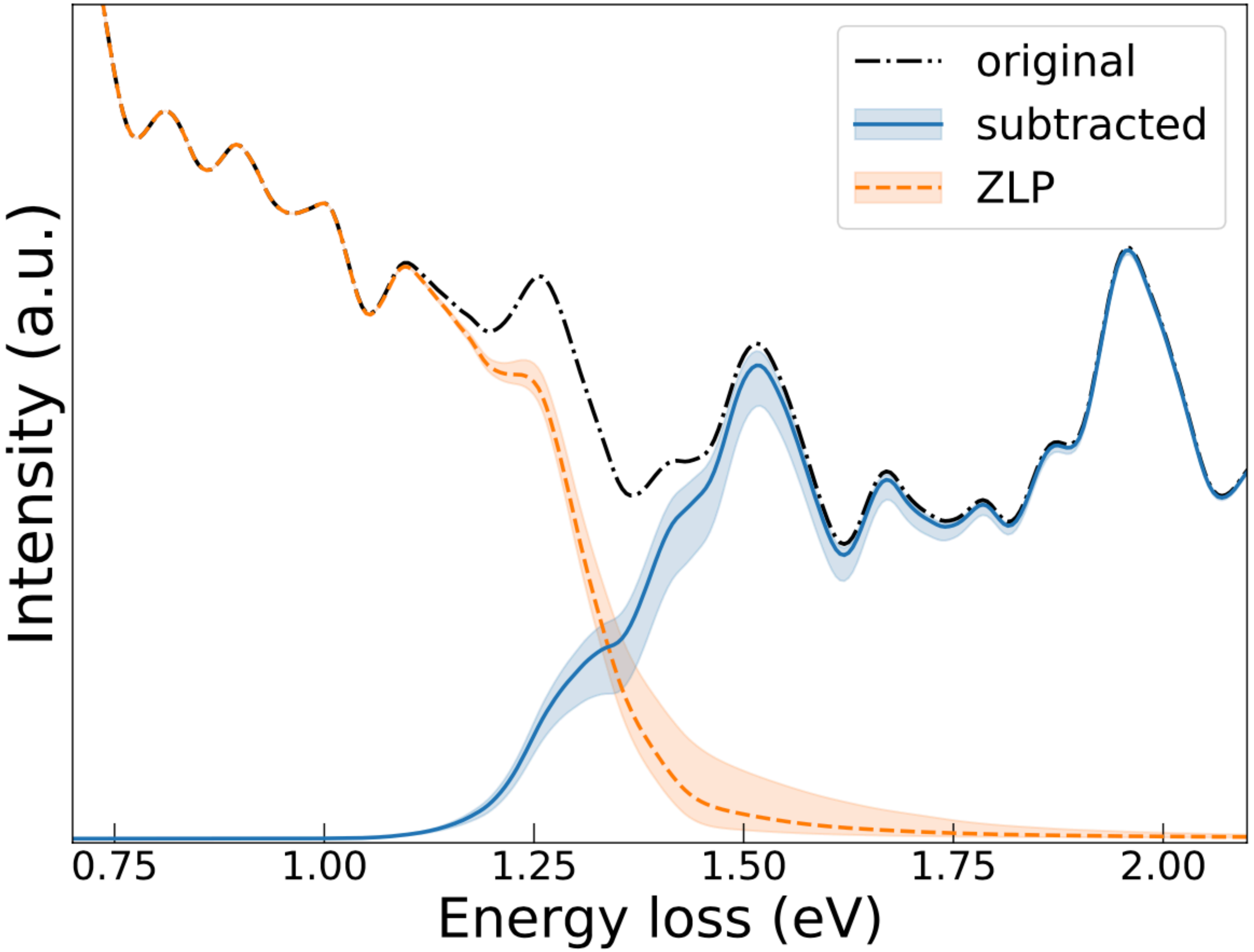

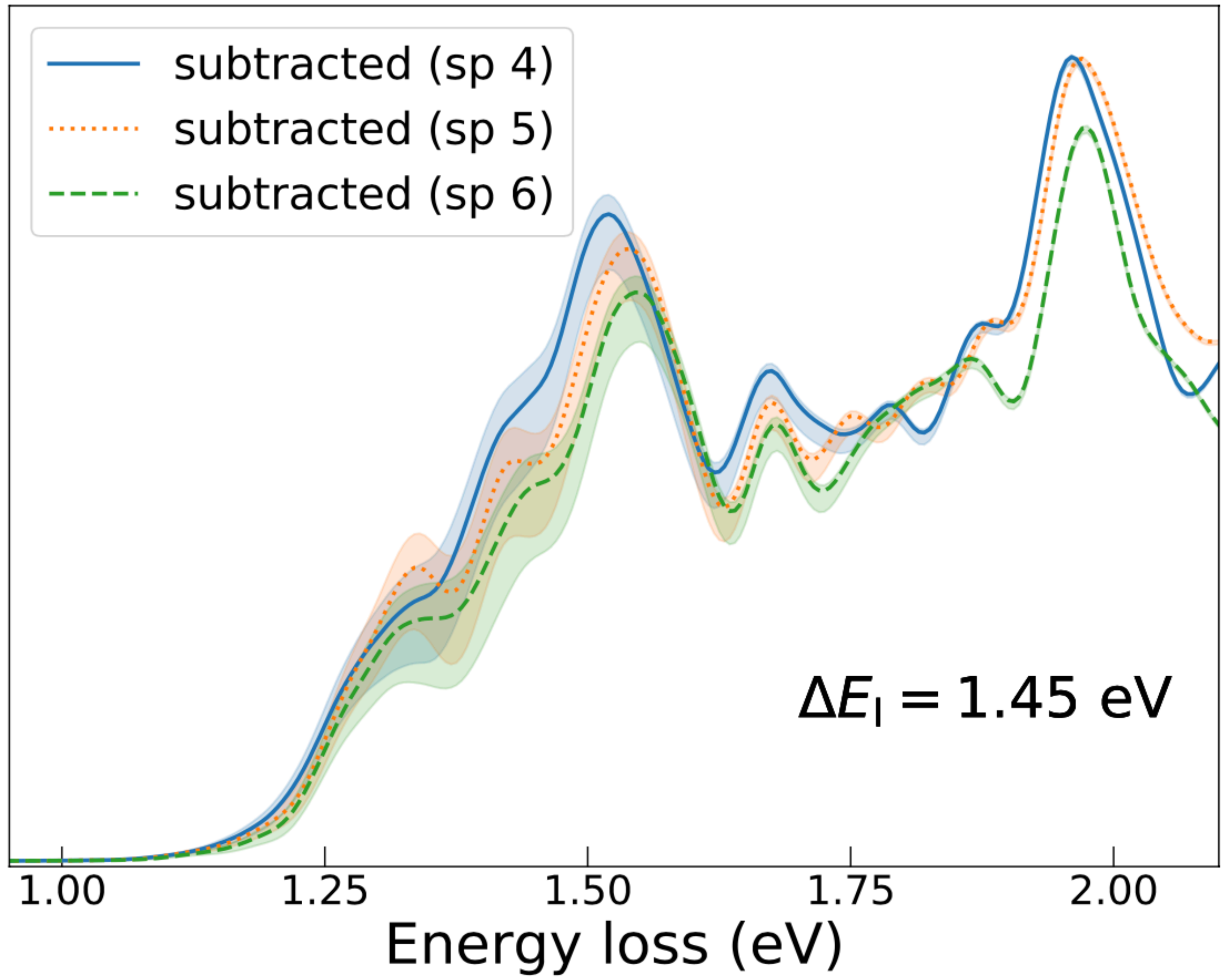

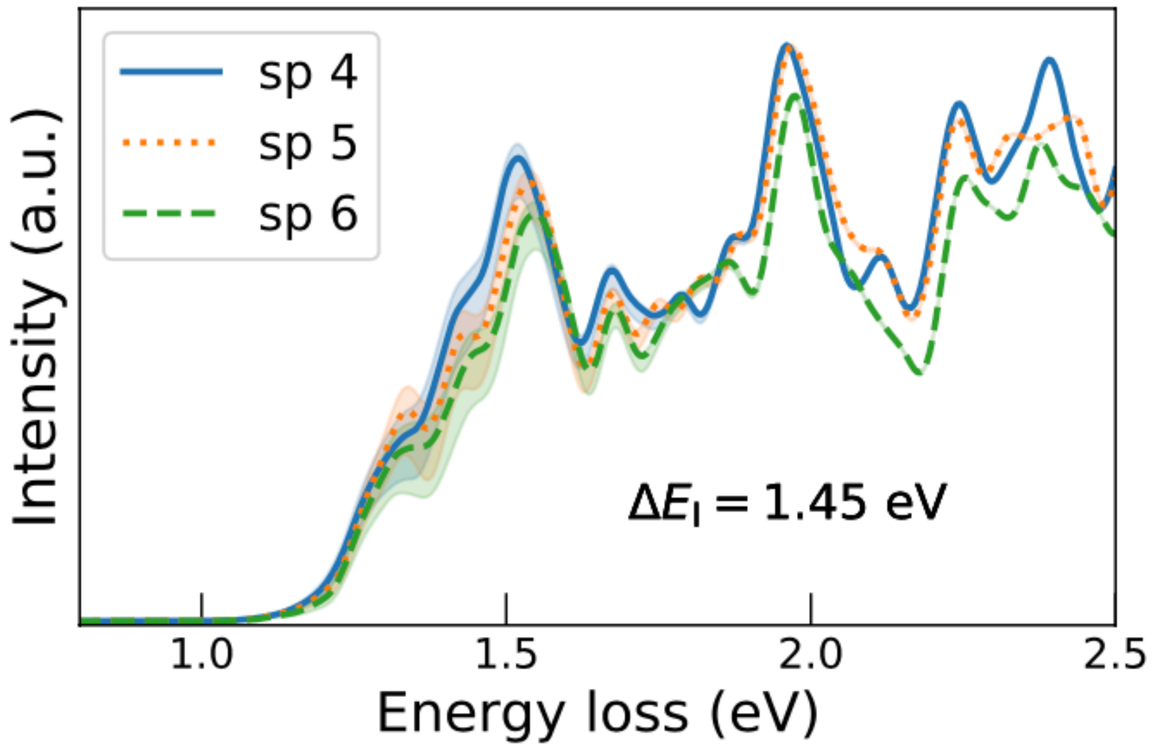

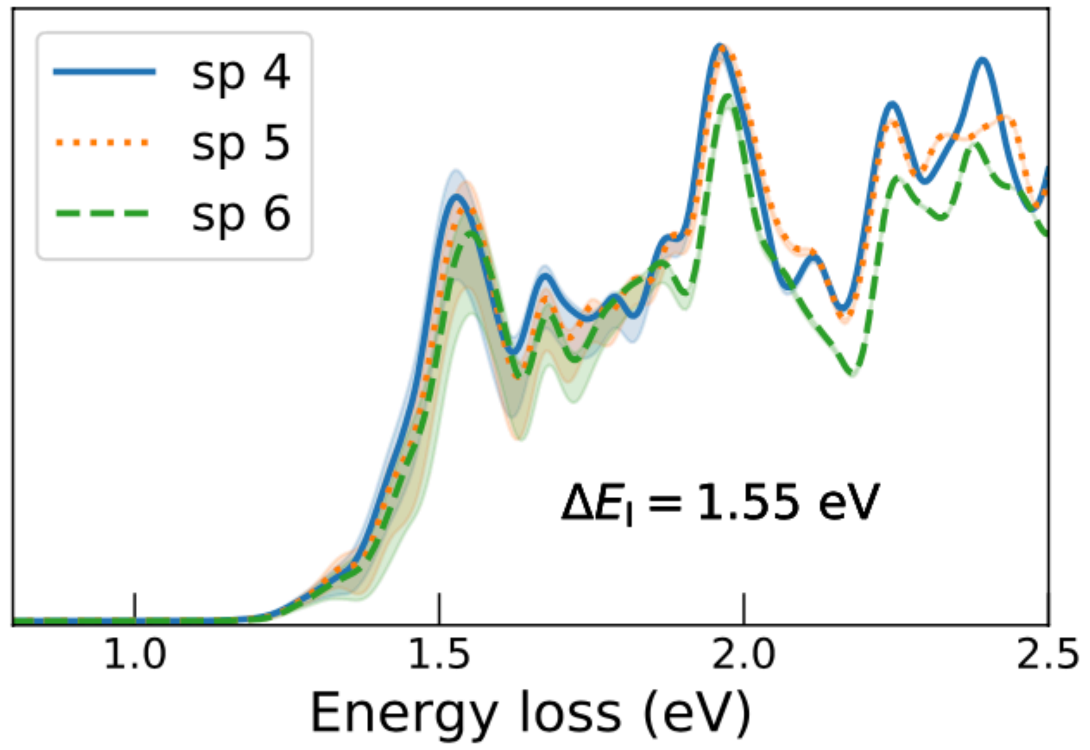

Conclusions and Outlook

Parametrization of the ZLP

- Reliable predictions
- Flexible model
- Error propagation

Subtraction of the ZLP

- Subtraction with uncertainties
- Different microscope parameters and sample thicknesses

- Include more operating conditions and verify extrapolation predictions

- Further explore low-loss region: phonon excitations?
- Apply to different nanostructures
- Fast and automated spectra readout
- Energy gain peaks

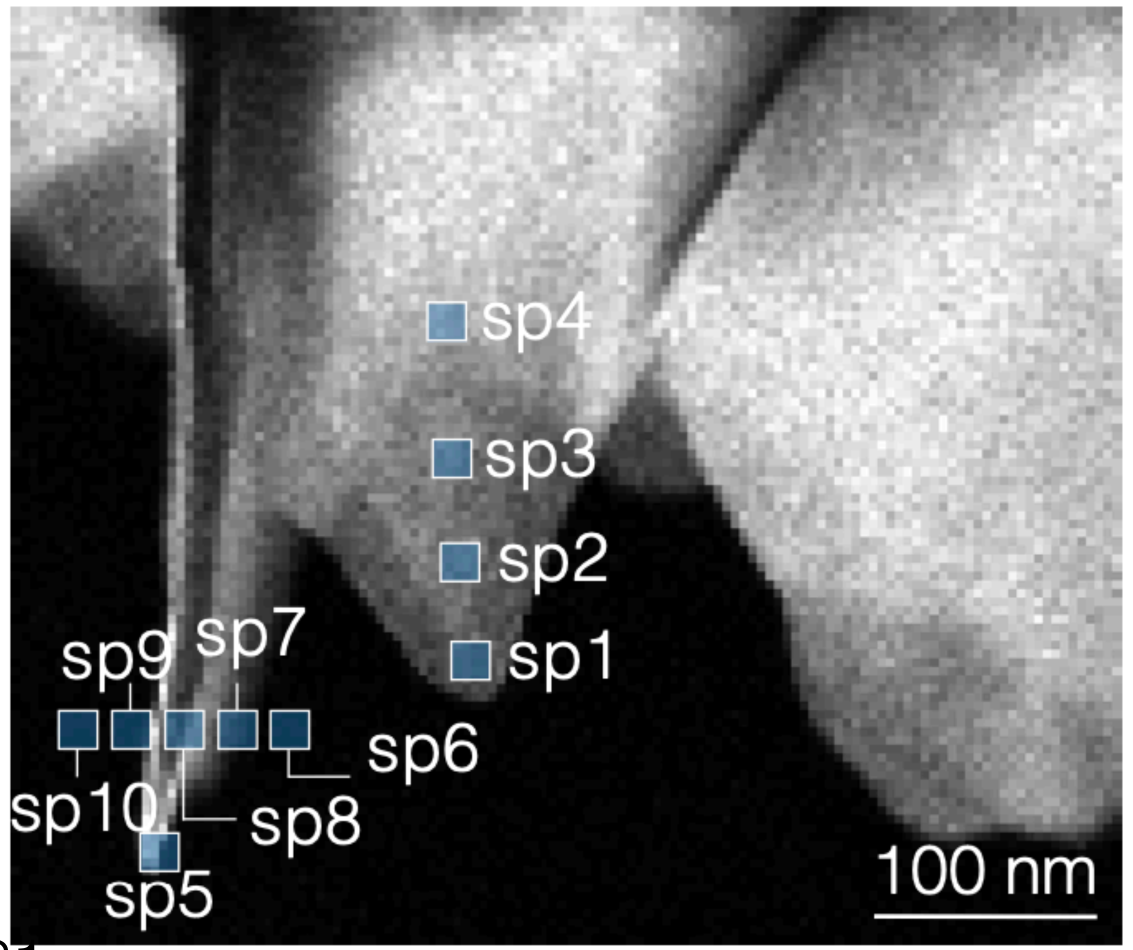

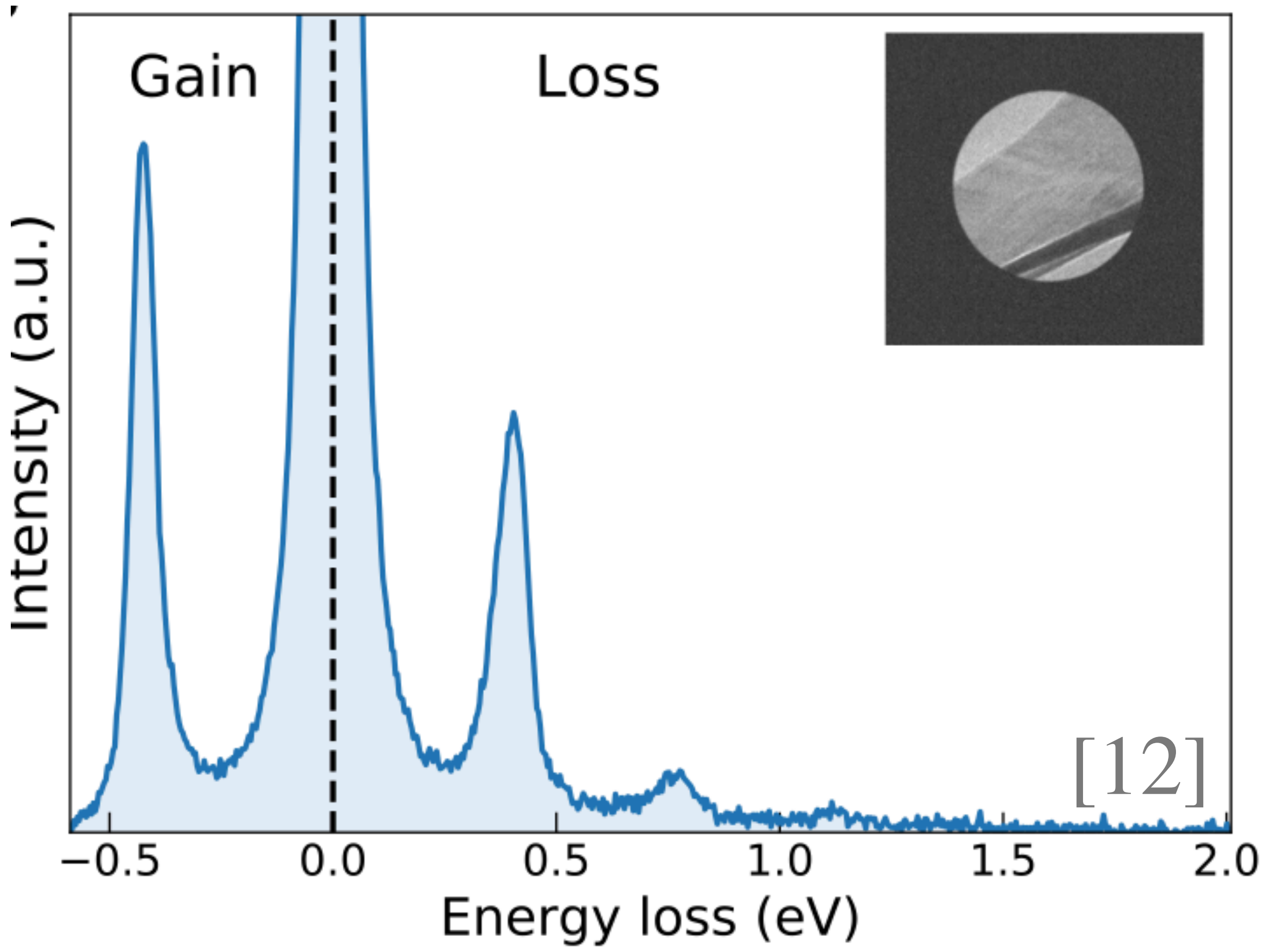

Charting the low-loss region in Electron Energy Loss Spectroscopy with machine learning

Laurien Roest

October 1st, 2020

Committee members:
Dr. S. Conesa-Boj Supervisor, TU Delft (QN)
Dr. E. Greplova TU Delft (QN)
Dr. Ir. J.P. Hoogenboom TU Delft (ImPhys)

References

1. SingularityHub
2. Jon Paul Johnson
3. Matmatch
4. jzjdm.com
5. E. Pomerantseva and Y. Gogotsi, *2D Hetero Structures for energy storage,* Department of Materials Science and Engineering
6. SemanticScholar
7. V. Yadav et. al. *2D MoS2-Based Nanomaterials for Therapeutic, Bioimaging, and Biosensing Applications.* Small **15** (2019).
8. A. Dorneich, R. French, H. Mullejans, et al., *Quantitative analysis of valence electron energy-loss spectra of aluminium nitride,* Journal of Microscopy **191** (1998) 286–296.
9. S. Lazar, G. Botton, et al., *Materials science applications of HREELS in near edgestructure analysis an low-energy loss spectroscopy,* Ultramicroscopy **96** (2003) 535–546.
10. R. Erni, N. D. Browning, Z. Rong Dai, and J. P. Bradley, *Analysis of extraterrestrial particles using monochromated electron energy-loss spectroscopy,* Micron **35** (2005) 369–379.
11. K. van Benthem, C. Elsässer, and R. French, *Bulk electronic structure of SrTiO3: Experiment and theory,* Journal of Applied Physics **90** (2001).
12. S. E. van Heijst, M. Masaki, E. Okunishi, H. Kurata, L.I. Roest, L. Maduro, J. Rojo, and S. Conesa-Boj, *Illuminating the electronic properties of WS2 polytypism with electron microscopy.* arXiv:2009.08477
13. J. Bruley and L. Brown, *Analytical Electron Microscopy Workshop*, The Institute of Metals, London, Edited by G.W. Lorimer (1987).

Supplementary materials

Neural network architecture

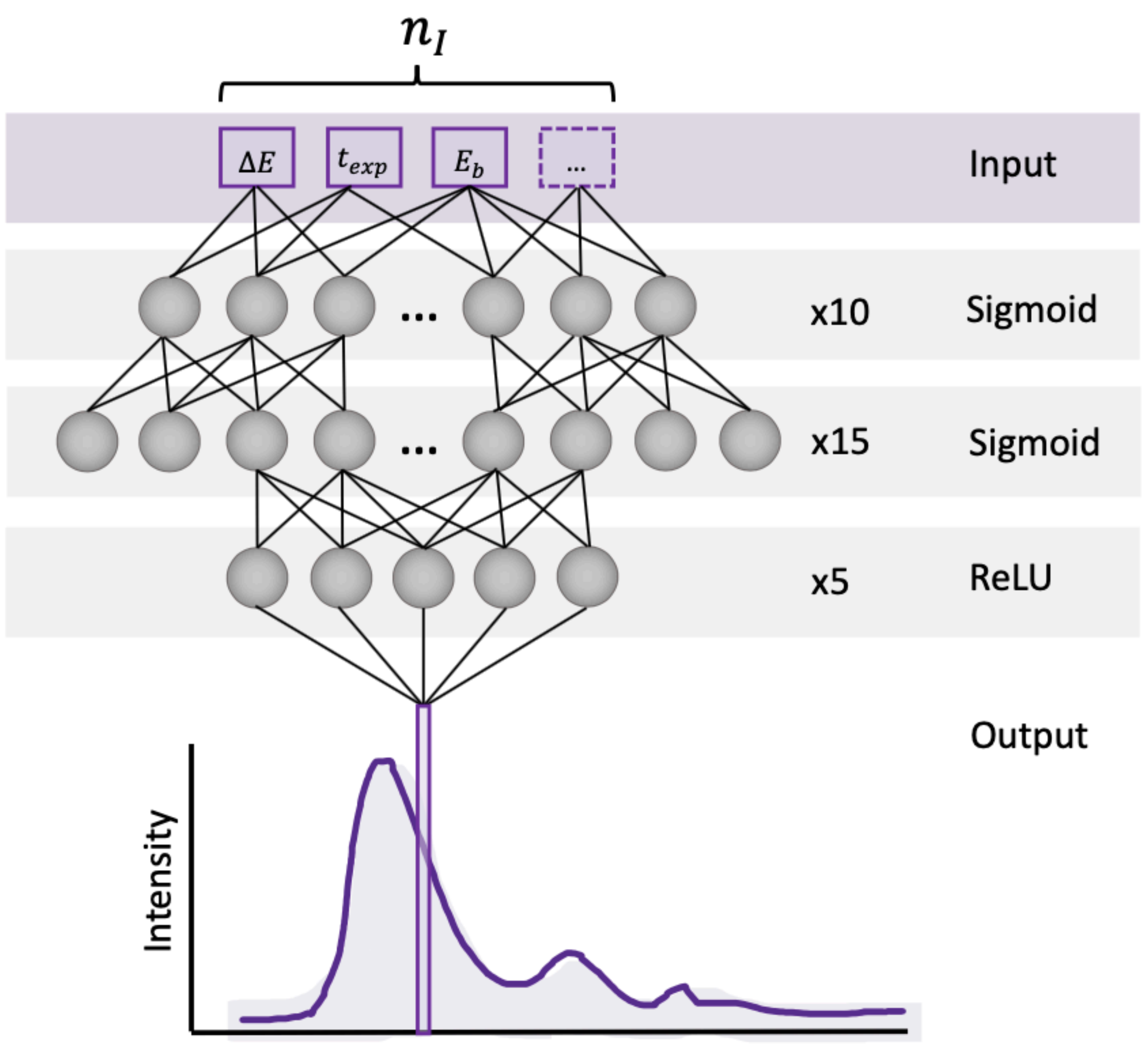

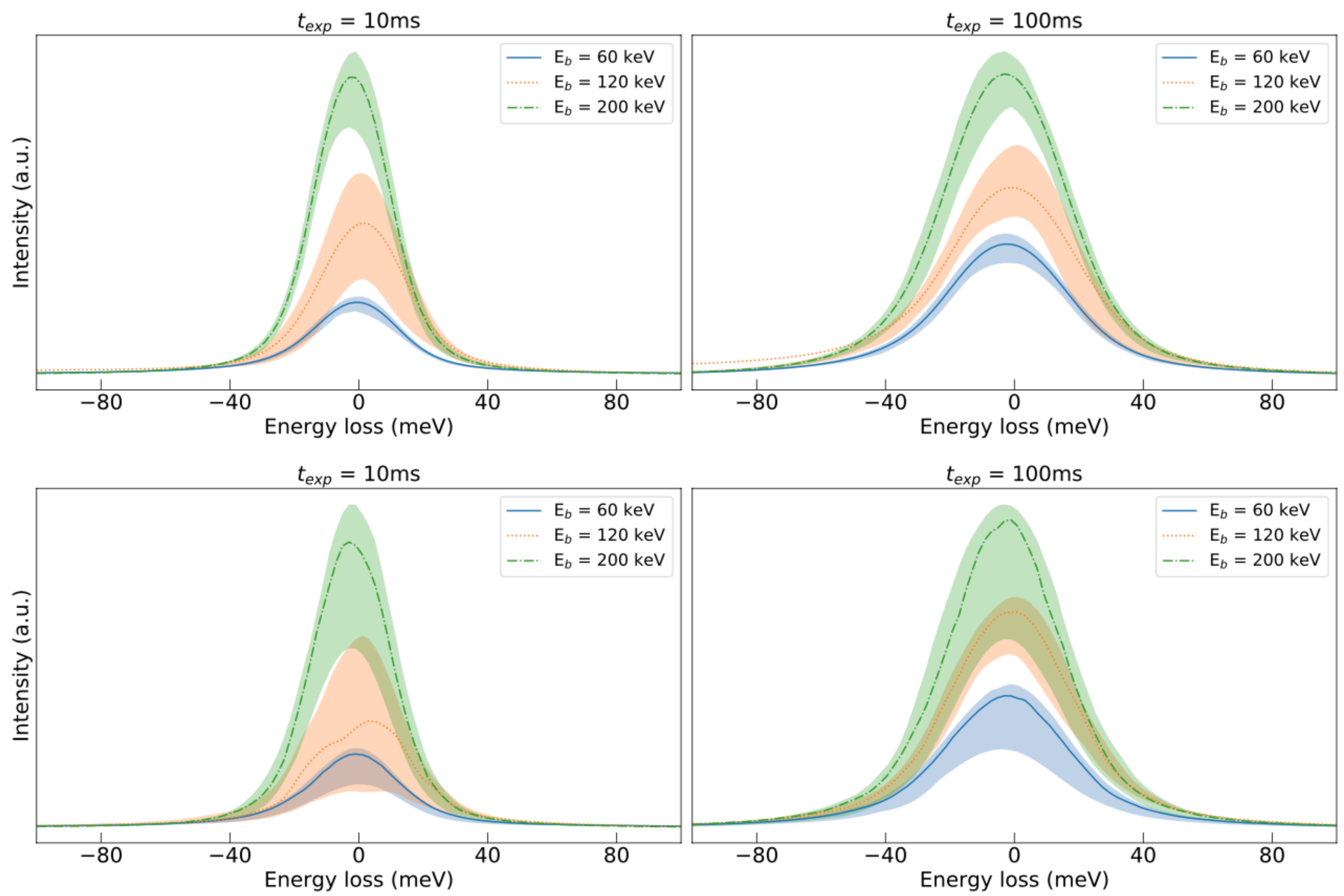

Supplementary materials

Spectra properties

Set	t_{exp} (ms)	E_{b} (keV)	N_{sp}	N_{dat}	ΔE_{min} (eV)	ΔE_{max} (eV)	FWHM (meV)
1	100	200	15	2048	-0.96	8.51	47 ± 7
2	100	60	7	2048	-0.54	5.59	50 ± 4
3	10	200	6	2048	-0.75	5.18	26 ± 3
4	10	60	6	2048	-0.40	4.78	34 ± 2

Set	t_{exp} (ms)	E_{b} (keV)	N_{sp}	N_{dat}	ΔE_{min} (eV)	ΔE_{max} (eV)	FWHM (meV)
A	1	60	6	1918	-4.1	45.5	470 ± 10
B	190	60	10	2000	-0.9	9.1	87 ± 5

Supplementary materials

Derivatives

Set	$\Delta E\|_{\min}$ (eV)	ΔE_{I} (eV)	ΔE_{II} (eV)
A	2.70 ± 0.06	1.8	12
B	1.80 ± 0.04	1.4	6

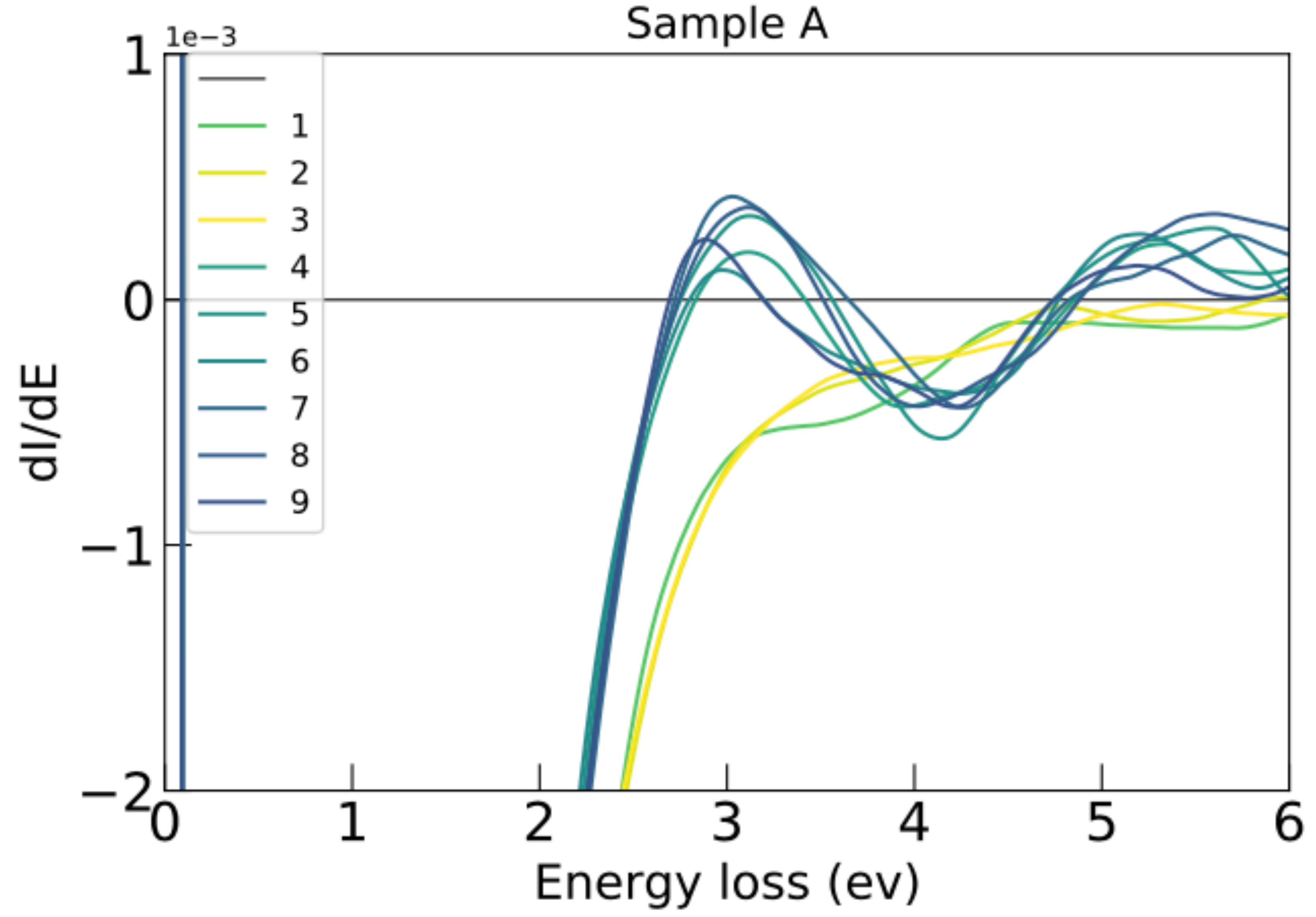

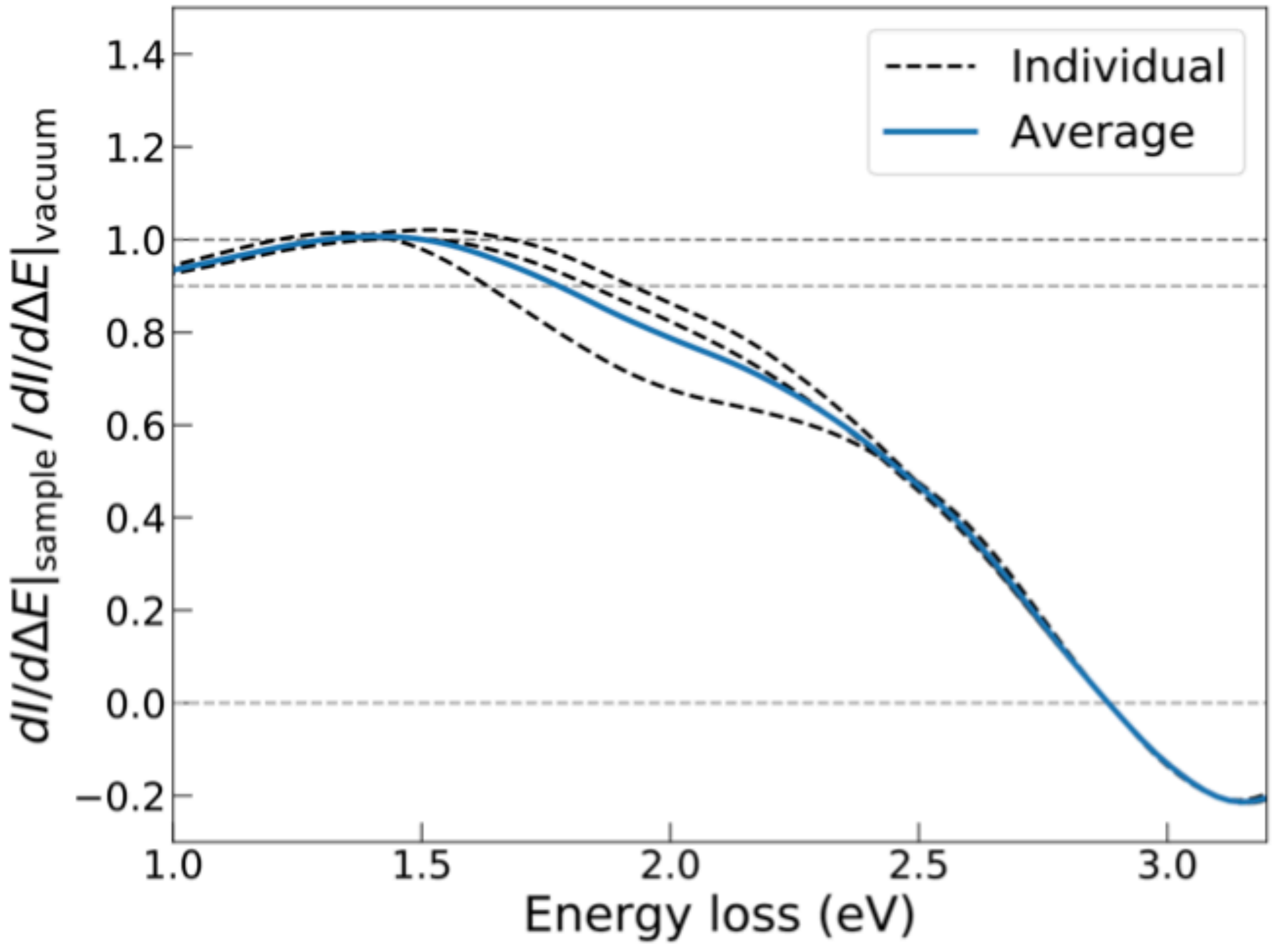

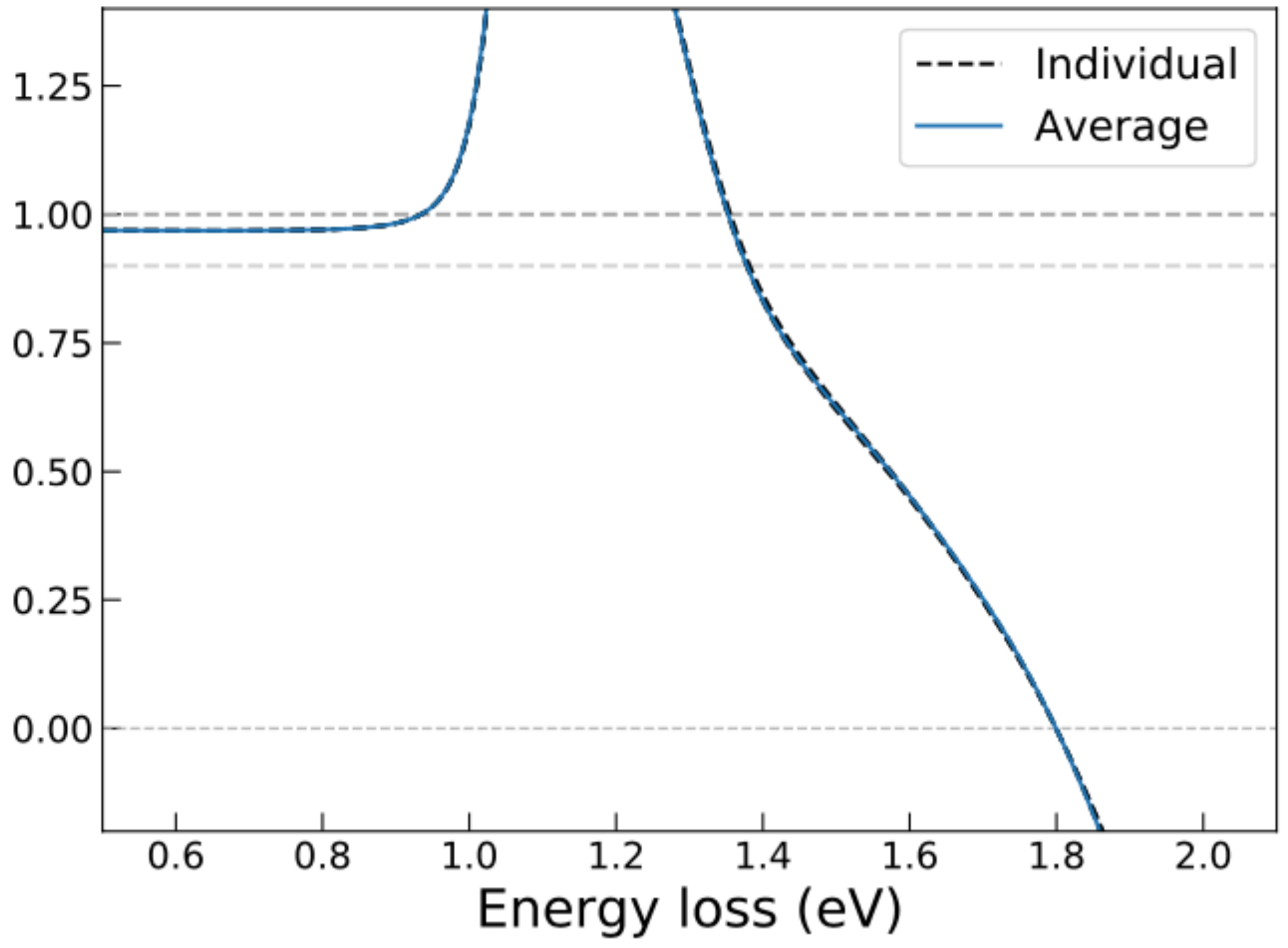

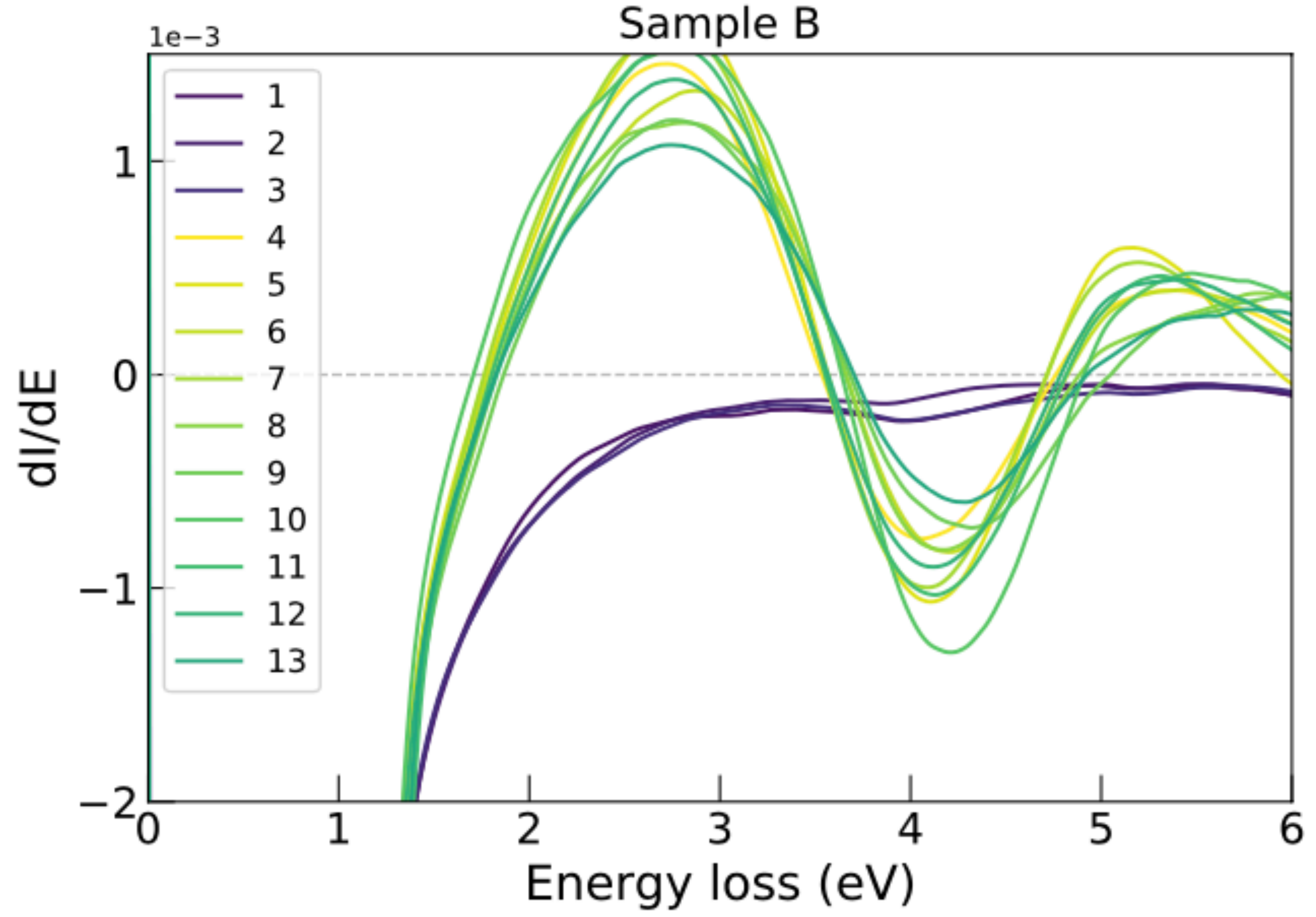

Supplementary materials

Sample A

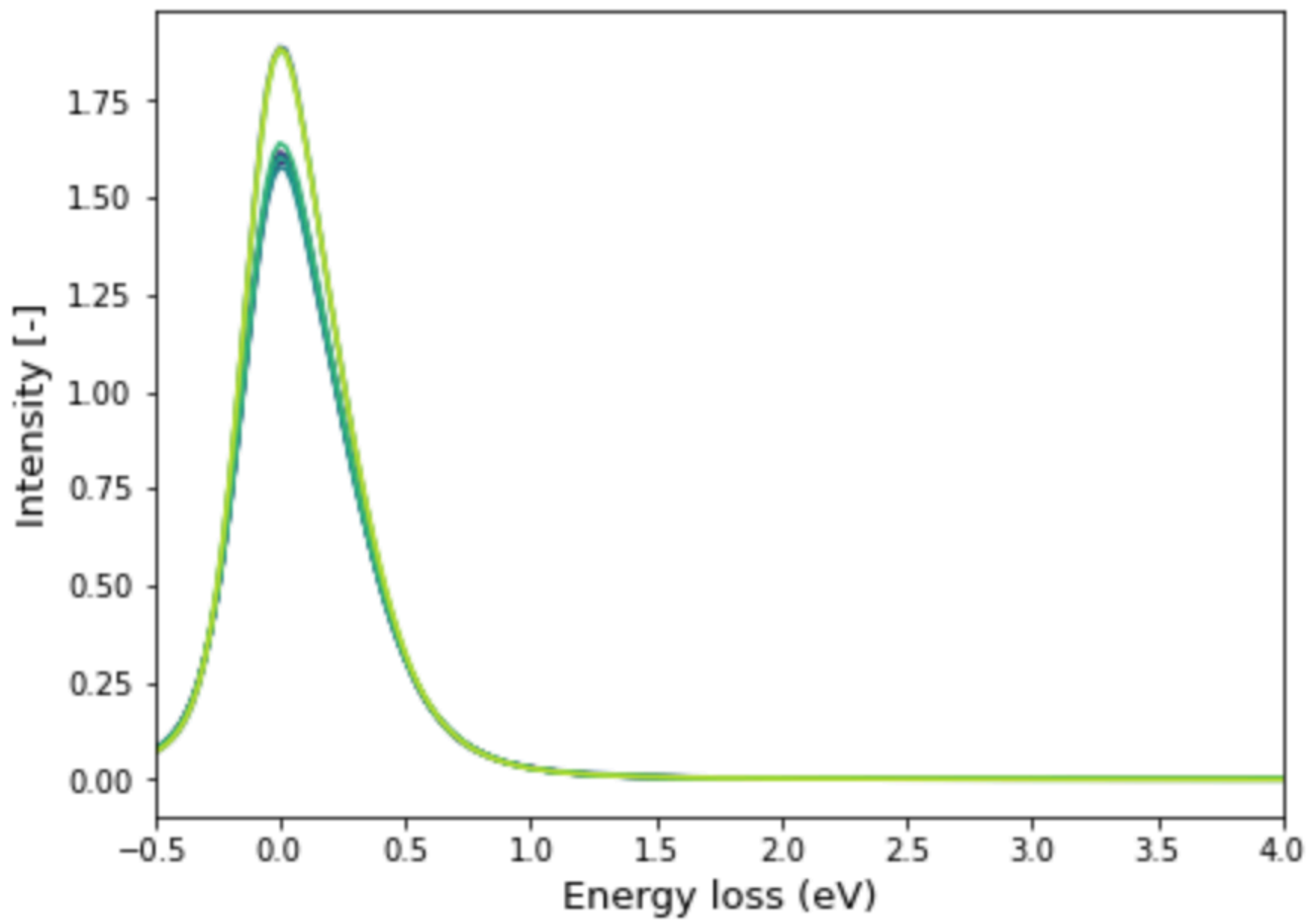

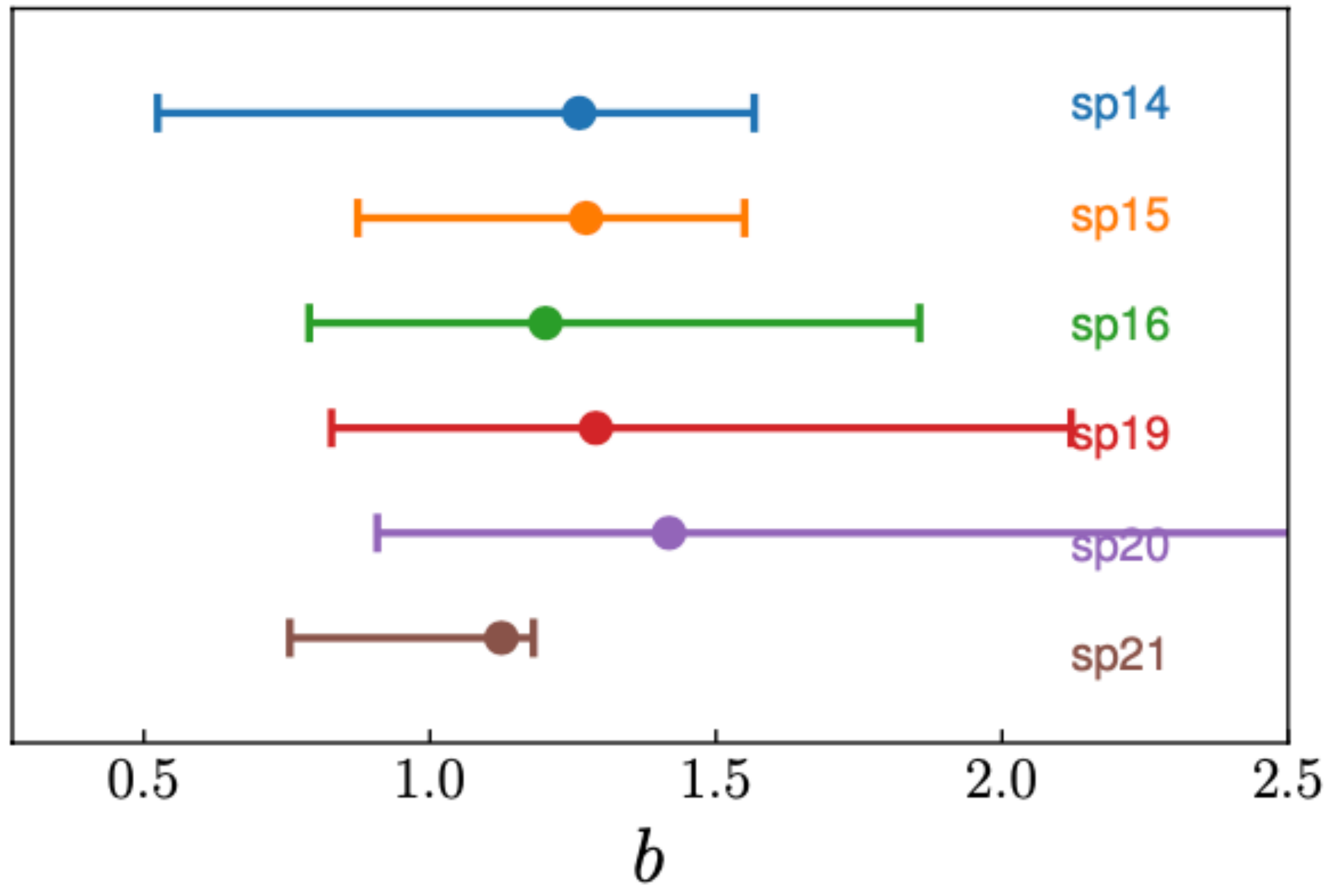

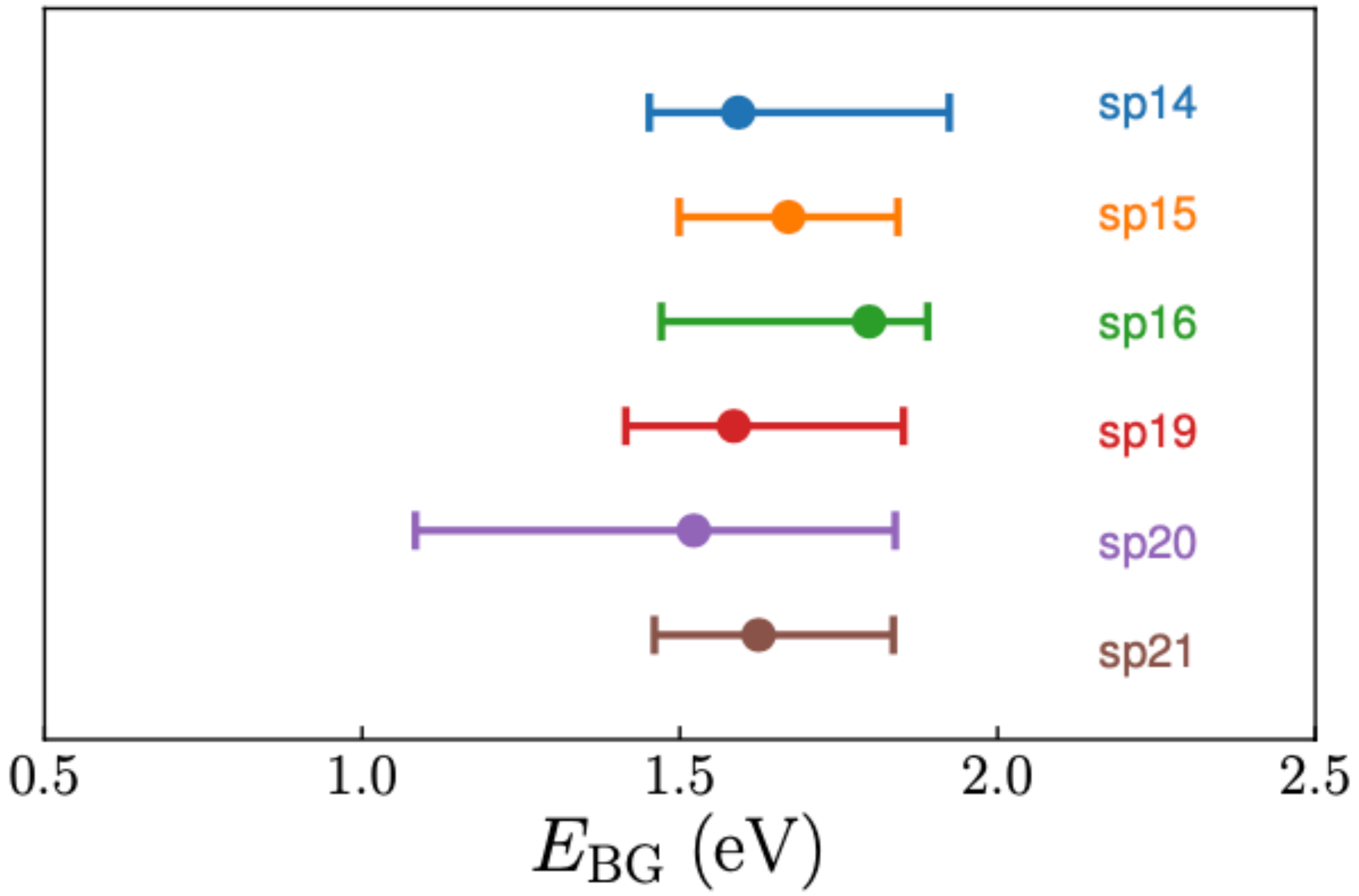

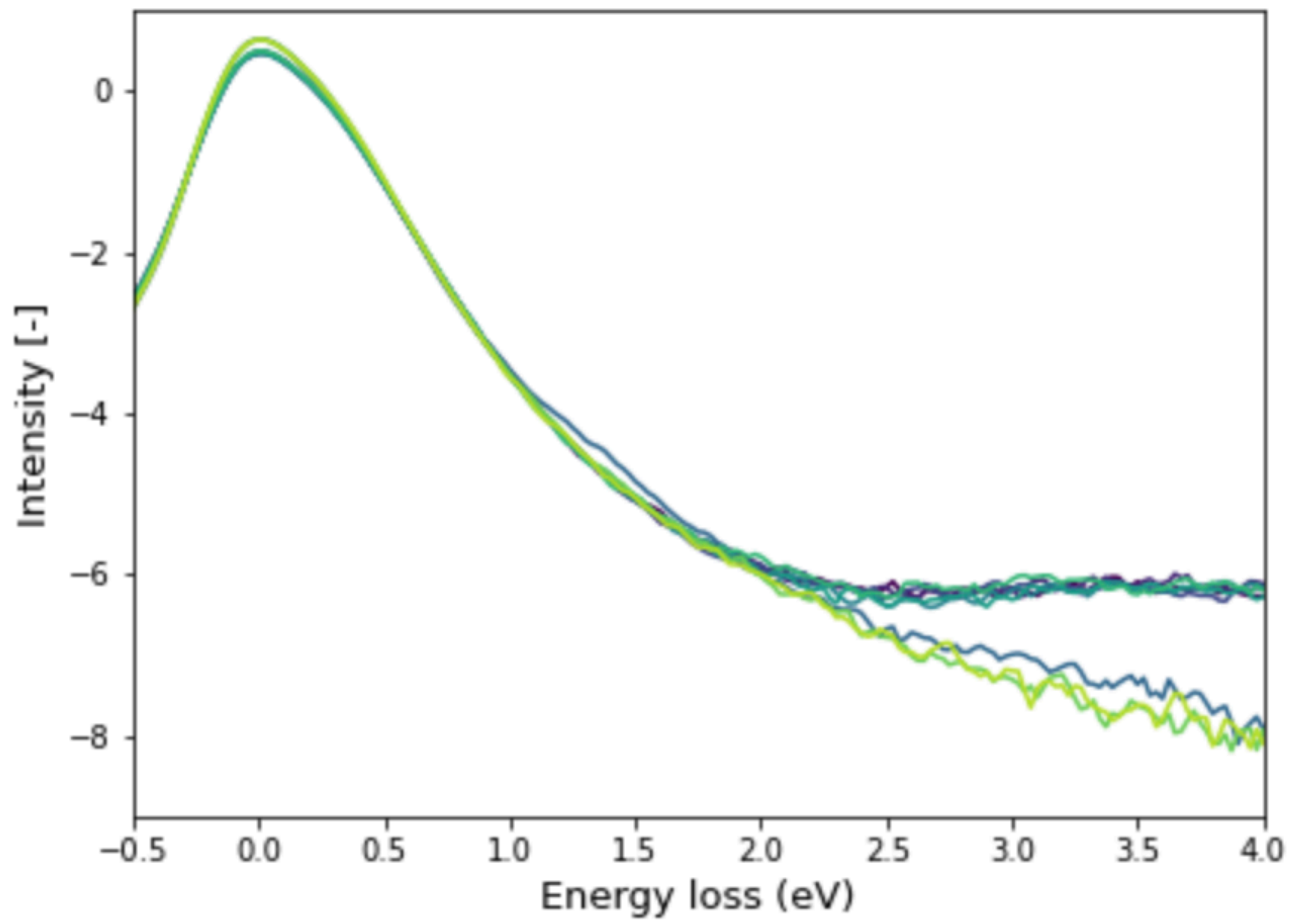

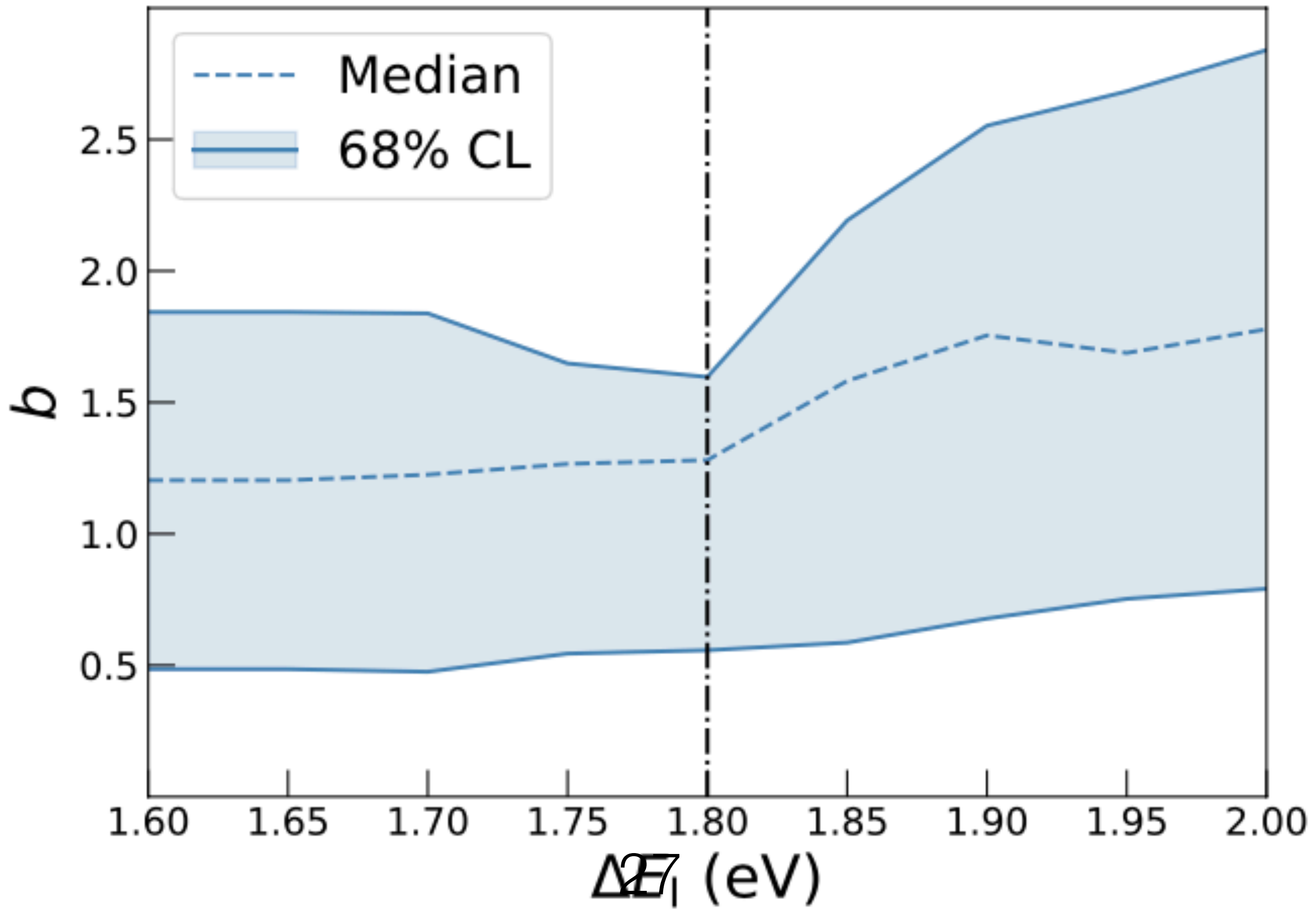

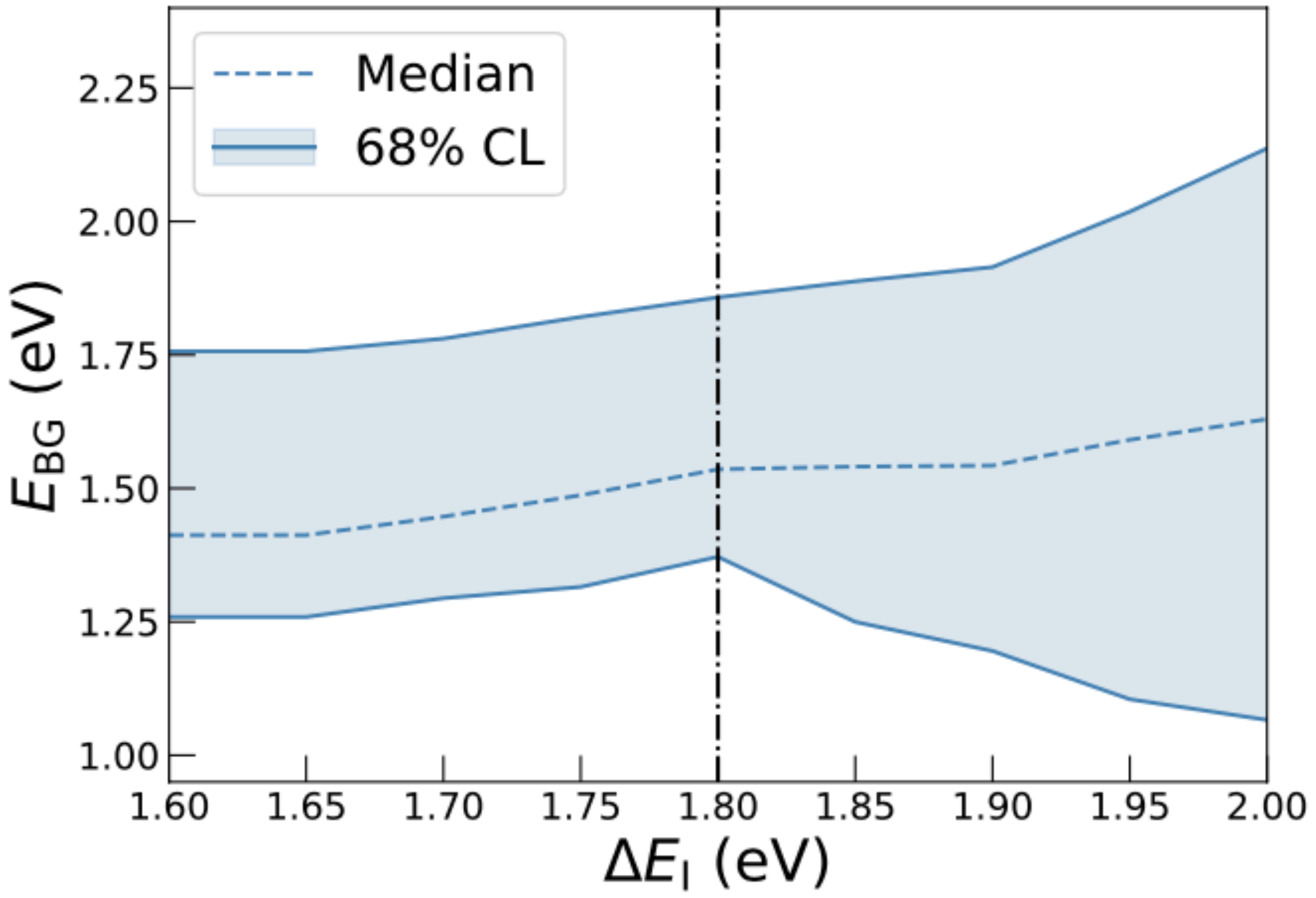

Supplementary materials

Bandgap values

Reference	Thickness	E_{bg} (eV)	Band gap type	Technique
[35]	bulk	1.4 ± 0.07	indirect	Gate-voltage dependence
[36]	ML	2.14	direct	Gate-voltage dependence
	bulk	1.40	indirect	
[37]	ML	2.03 ± 0.03	direct	DFT
	bulk	1.32 ± 0.03	indirect	
[38]	ML	1.76 ± 0.03	direct	Absorption edge coefficient fitting
	bulk	1.35	indirect	
[39]	ML	2.21 ± 0.3	direct	Bethe-Salpeter equation (BSE)

Table 2.1. Representative results for the determination of the bandgap energy E_{bg} and its type in WS_2, obtained from a variety of experimental and theoretical techniques. For each reference we indicate separately the bulk results and those obtained for monolayers.

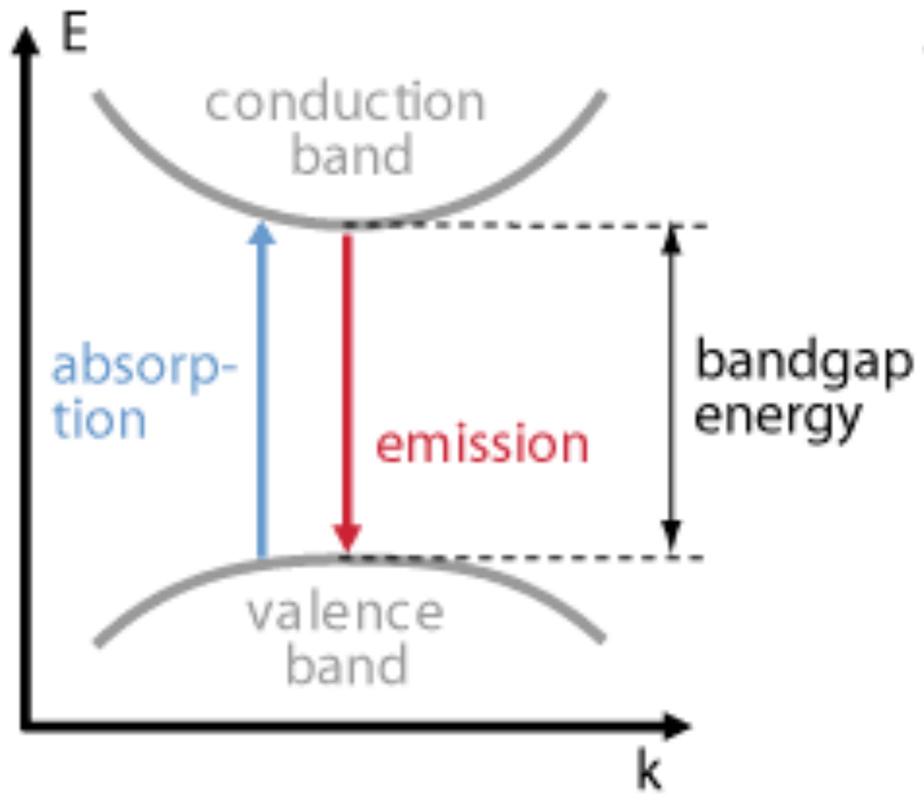

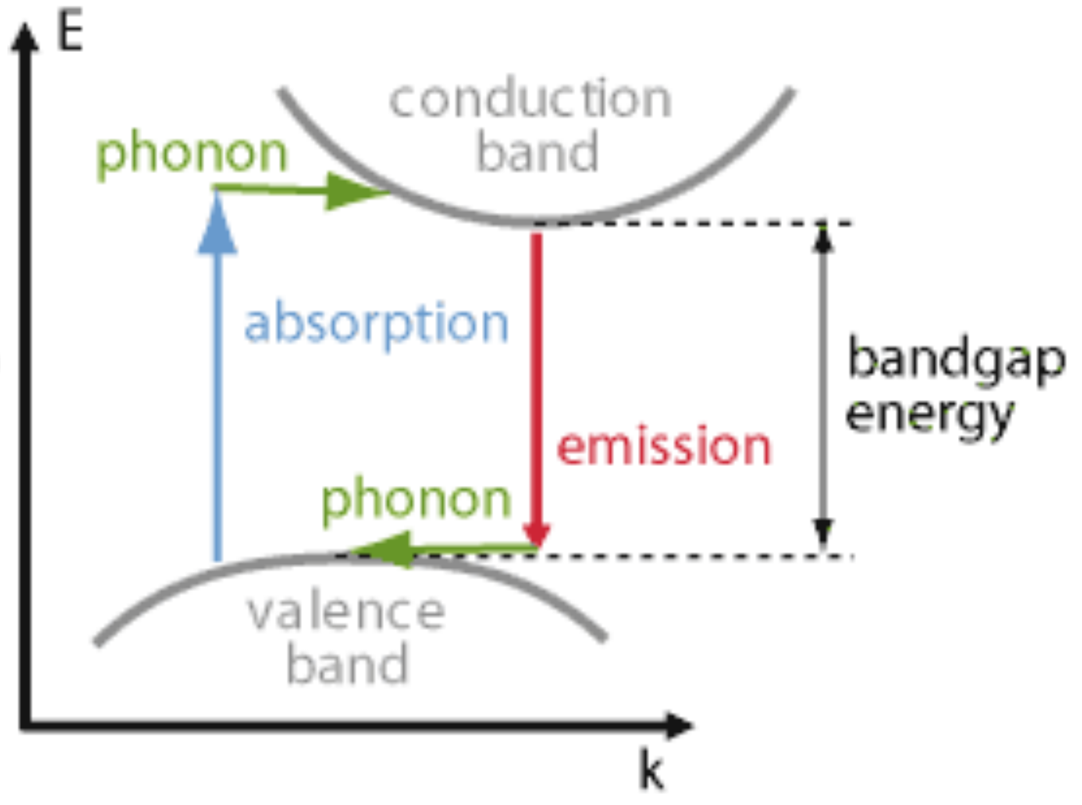

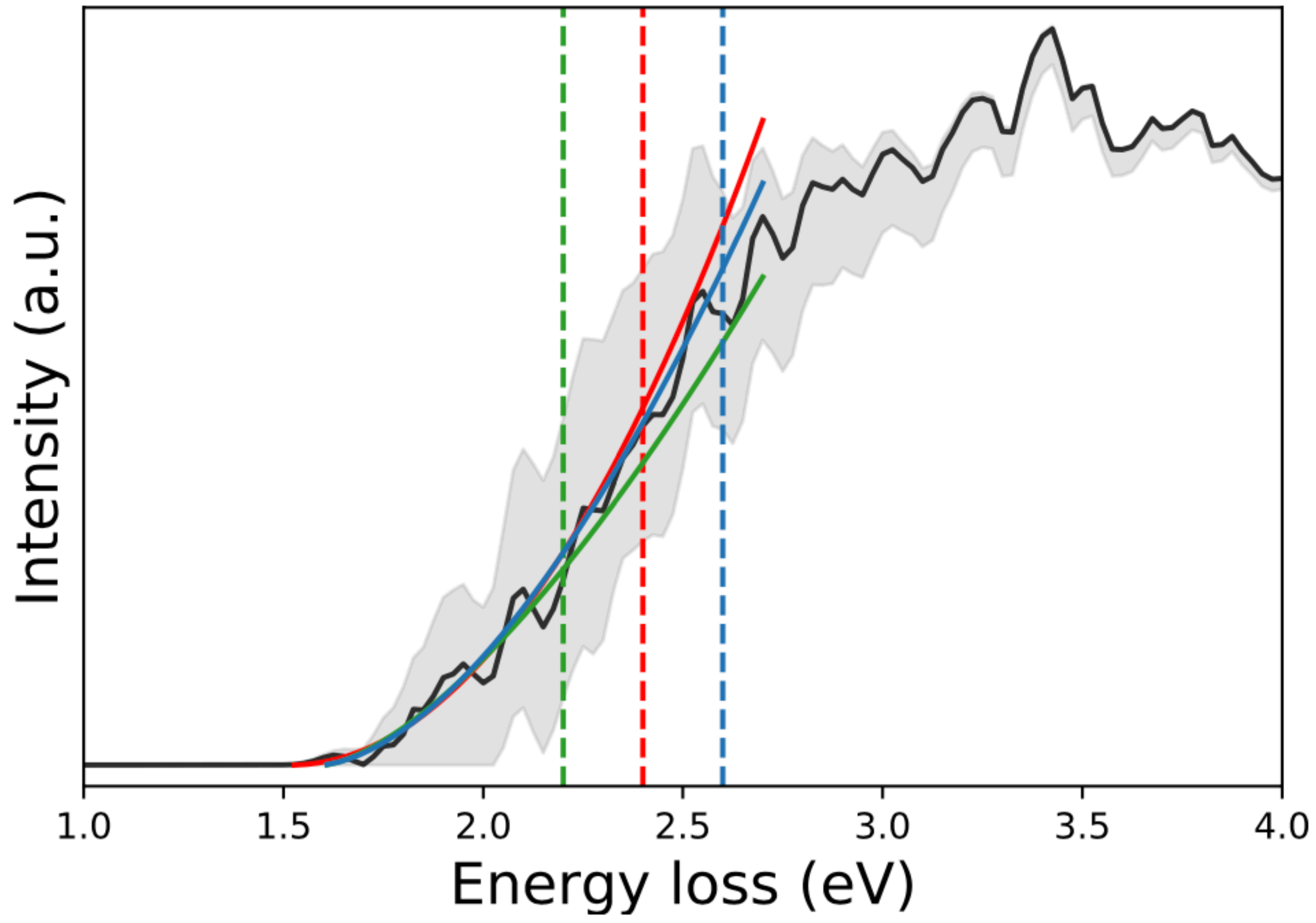

Supplementary materials

Sample B